Identification of Source Faults of Large Earthquakes in the Turkey-Syria Border Region Between AD 1000 and the Present, and their Relevance for the 2023 M_w 7.8 Pazarcık Earthquake

S. Carena[1], A. M. Friedrich[1], A. Verdecchia[2], B. Kahle[1,3], S. Rieger[1], and S. Kübler[1]

[1]Department of Earth and Environmental Sciences, Ludwig-Maximilians-Universität München, Munich, Germany.

[2]Institute for Geology, Mineralogy and Geophysics, Ruhr-Universität Bochum, Bochum, Germany.

[3]Department of Geological Sciences, University of Cape Town, South Africa.

Corresponding author: Sara Carena (scarena@iaag.geo.uni-muenchen.de)

Key Points:

- We identified the source faults of fourteen large earthquakes along the East Anatolian and northern Dead Sea fault systems
- Maximum magnitude for the East Anatolian fault zone is approximately 8.2
- Continental transforms may be described as having a collective memory

Abstract

The February 6th, 2023, M_w 7.8 Pazarcık earthquake in the Turkey-Syria border region raises the question of whether such a large earthquake could have been foreseen, as well as what is the maximum possible magnitude (M_{max}) of earthquakes on the East Anatolian fault system and on continental transform faults in general. To answer such questions, knowledge of past earthquakes and of their causative faults is necessary. Here, we integrate data from historical seismology, paleoseismology, archeoseismology, and remote sensing to identify the likely source faults of fourteen $M_w \geq 7$ earthquakes between AD 1000 and the present in the region. We find that the 2023 Pazarcık earthquake could have been foreseen in terms of location (the East Anatolian Fault) and timing (an earthquake along this fault was if anything overdue), but not magnitude. We hypothesize that the maximum earthquake magnitude for the East Anatolian Fault is in fact 8.2, i.e. a single end-to-end rupture of the entire fault, and that the 2023 Pazarcık earthquake did not reach M_{max} by a fortuitous combination of circumstances. We conclude that such unusually large events are hard to model in terms of recurrence intervals, and that seismic hazard assessment along continental transforms cannot be done on individual fault systems but must include neighboring systems as well, because they are not kinematically independent at any time scale.

Plain Language Summary

On February 6th, 2023, there was a magnitude 7.8 earthquake in the Turkey-Syria border region. It surprised many people, including many Earth scientists, because of where it happened (on the East Anatolian fault) and because of how large it was. People wondered whether it could have been foreseen, and how large an earthquake on this fault can really be. To figure this out, we looked at the history of earthquakes in the region in the last 1000 years. We used information from historical seismology, paleoseismology, archeoseismology, and remote sensing to identify the faults that caused fourteen earthquakes with magnitude 7 or greater in this region. We found that the location (East Anatolian Fault) and timing (it was due any time) of the 2023 earthquake were foreseeable, but not the magnitude. In fact, we believe that the maximum magnitude for the East Anatolian Fault is 8.2, and that the 2023 earthquake was below this maximum just by accident. It is hard to say how often such large events can happen, because many different things need to align. We also believe that it is

necessary to look at neighboring fault systems when estimating seismic hazards, because they interact.

1 Introduction

The occurrence of the Feb. 6th 2023 M_w 7.8 Pazarcık earthquake surprised not only the public, but also a large part of the geoscience community, due to the event size and location. This earthquake ruptured ~310 km of the left-lateral East Anatolian Fault (EAF) between Antakya and Çelikhan (Figure 1), which is ~55% of its length. It also ruptured through multiple segment boundaries (Figure 2). The EAF had been, until February 2023, a plate boundary fault largely overlooked by the international community, with the great majority of works since about 1970 mainly dealing with the North Anatolian Fault (NAF) because of its proximity to Istanbul and of its higher level of seismic activity in the past century. Publications about the NAF are on average ~ 6 times more numerous than those about the EAF (Table 1). Even the most recent earthquake on the EAF, the Jan. 24th 2020 Elâziğ M_w 6.8 event, received surprisingly little attention. As of July 2023, there were only 10 geoscience papers about this earthquake listed in Web of Science. For comparison, the 1999 Düzce earthquake along the NAF had 13 papers listed in the same database over the first 3 years after the event, even though publishing rates have increased rapidly over time.

The EAF, however, has been documented as seismically very active in historical records, with magnitudes above 7.0 inferred for multiple earthquakes around the EAF in the past 1000 years (e.g. Ambraseys, 1989, 2009; Guidoboni & Comastri, 2005; Sbeinati et al., 2005; Meghraoui, 2015). For most of these earthquakes, though, the specific source faults were either not identified, or identification from different authors varies considerably, or it lacks documentation. Lack of knowledge of source faults precludes the calculation of fault slip rates and recurrence times, and the estimation of seismic hazards and M_{max}. It also precludes having a rigorous base for stress and strain modeling and for studying dynamic rupture propagation.

Our goal is therefore to systematically identify the most likely source of each large ($M_w \geq 7.0$) earthquake along the East Anatolian and Dead Sea fault systems between Lake Hazar in the north and Qalaat El Hosn, Syria, in the south (Figure 1) in the past ~1000 years, because these earthquakes may have had a direct and significant influence on the timing, location, and size of the 2023 M_w 7.8 Pazarcık earthquake. The more recent an earthquake is,

the more likely it is to have been the "last event" on its source fault, determining the last coseismic and postseismic stress changes associated with the fault itself. Before AD 1000 the historical records are in any case very fragmentary, making it impossible to associate most earthquakes with a specific fault. By integrating historical records with paleoseismological ones in a tectonic context, we aim to identify a set of reasonable fault / earthquake pairs and any plausible alternatives that can be used for both modeling purposes and the identification of key field sites for further studies.

2 Method and Results

The identification by previous authors of source faults of historical earthquakes along the EAF and northern Dead Sea Fault zone (DSF) is patchy. The typical case is, for example, when a historical seismology work assigns an earthquake to a fault simply on the basis that it is a known active fault in the general epicentral area. Often the source faults identified in this way are then reported by later authors without any critical re-evaluation, even in those cases when the original author had clearly stated that they were just doing a "best guess" approach with no additional data. In most cases each work identifies one or two earthquake / source pairs, or identifies multiple earthquakes, but all on the same fault. Unfortunately, identifying source faults in isolation or without looking at all data available in both time and space is more likely to result in mis-identification, the more so the older the earthquake is. We have therefore started from published historical seismology works, re-evaluating each piece of information from different authors about the same earthquake, and combining this with data from paleoseismology and remote sensing (often more recent), following the approach suggested by Daëron et al. (2007) for future studies on the DSF. We have not developed new methods, software, or collected field data. Rather, we have carried out a comprehensive review of the information that already exists and attempted to weed out inconsistencies and integrate information from different fields. Finally, when reviewing information, we have done so for several earthquakes and faults simultaneously, when these are (or could be) in the same sub-region.

2.1 Identification of source faults

In the case of the Turkey-Syria border region, several of the faults have been trenched, so several events from the past 1000 years can be assigned to a specific fault with a

reasonable degree of confidence. In some cases, a couple of different options are equally plausible but, overall, there is a limited combination of possible earthquake / source-fault pairs, because there is only a limited number of faults in the area that are long enough to be credible source faults for events of M_w 7 and above. We will start our analysis from those earthquakes for which there is the most information available, and which may appear in one or more of the trenches, then move to events which are less well-constrained. The order is not going to be strictly chronological, because some of the older events are well-constrained, and some of the more recent ones are not. We are going to start from the Amik basin area (Figure 1a), where the EAF and DSF come together, and move first south and then north. The final list of earthquake / fault pairs that we have determined to be the most likely can be found in Table 2, and the faults are shown in Figure 2b.

There are a few criteria that can be applied to the identification of the likely source fault of a historical earthquake in the absence of dating of geological or archeological features: (1) empirical relationships (e.g. Wells & Coppersmith, 1994) between earthquake size and fault parameters (a large earthquake must have a long rupture, so determination of epicenter position alone is not very meaningful), (2) the principle, based on Coulomb stress theory, that the same fault segment or neighboring parallel faults (i.e. side-by-side) with the same kinematics are highly unlikely to produce two large earthquakes within a few years or even decades of each other, and (3) careful reading of earthquake effect descriptions, paying particular attention to discussions by previous authors concerning reliability of sources. The latter is especially important because it is not uncommon for mistakes to be spread from one earthquake catalog to the next (or newly introduced) when information is accidentally left out, or two smaller earthquakes are conflated into a larger one.

A new source of information that we have today, which was not available when all the work on historical earthquakes in this region was being carried out, is the occurrence of the 2023 M_w 7.8 and 7.5 Turkey / Syria earthquakes (M_w from U.S. Geological Survey, 2023), which allowed us for example to verify that the empirical relationship used by previous authors to estimate magnitudes for historical earthquakes in this region is indeed appropriate (see Appendix A for details). This earthquake is also invaluable in that it shows how fault segmentation can be overcome to produce a very large earthquake, i.e. we should not fall into the trap of automatically assuming a rupture cannot propagate past a bend or step when examining historical earthquakes.

All the earthquakes that we consider are between AD 1000 and 2023, so "AD" is mostly omitted throughout the paper. As no year has two earthquakes, throughout the text for simplicity we only refer to the year of occurrence, omitting day and month. The precise date of each earthquake (when known) is given in Table 2. Due to the fact that locality names and fault names are very much relevant in this kind of work, in addition to the maps in Figure 1 we have supplied details of naming (including rationale for specific choices) in Appendix B, and a full searchable list of locality names with alternates as supplementary file ds04. Finally, as the number of place names is quite large, we will not call a figure every time a place is mentioned: this paper should be read with Figures 1 and 2 at hand at all times.

2.1.1 Amik basin and Dead Sea fault zone

We now apply the criteria described above to the earthquakes of 1872 and 1822. We start with this pair because the 1822 earthquake was singled out by Ambraseys (1989) not only as one of the largest earthquakes in the records, but also as one that took place in a region that - until February 2023 - had very low seismicity.

Altunel et al. (2009) attributed the last event in their trenches at Demirköprü (Figure 3, dated to between 1801 and 1940) to the 1872 earthquake based on their interpretation of Ambraseys's 1989 paper: "*Ambraseys (1989) reported that the 1822 earthquake took place in the Karasu Valley located further north of the Amik Basin […] it is therefore unlikely that the event E1 can be related to the 1822 earthquake. Ambraseys (1989) also reports that the 1872 April 3 earthquake was responsible of heavy damage north and south of the former Amik Lake, and in particular […] around Qillig and Armenez. On the basis of both paleoseismic results and historical accounts, we suggest that event E1 in trenches is related to the 1872 earthquake*". Ambraseys (1989), however, in the very next sentence to the one rephrased by Altunel et al. (2009) also states (concerning the Qillig area and the 1872 earthquake): "*Here, it is said, the earthquake split the ground in places and yellow sand filled the area, a description suggesting widespread liquefaction*". Liquefaction can happen at large distances from a fault surface rupture (Ambraseys, 1988; Papathanassiou et al., 2005), so evidence of liquefaction is not evidence for surface rupture at or near liquefaction location. In 2023, the M_w 7.8 earthquake caused liquefaction in Kumlu (Quillig) and many other localities in the southern and eastern Amik basin, even though the fault rupture was along the Amanos mountains front, and liquefaction was reported also from localities up to at least 40

km away (Taftsoglou et al., 2023). Furthermore, Ambraseys (1989) continues by writing, about the 1872 event: "*Also, between Batrakan and Qaralu, the valley to the east of the hills is said to have dropped […] and the ground was "rent" all the way to Baghras, an allusion to faulting*". The last three localities mentioned are at the foot of the Amanos mountains, about 20 km apart along the mountain front, and 18 km west of the trench site (Figures 1b and 3). Finally, the presumed location of the epicenter of the 1822 event has no bearing on whether the source fault can or cannot pass through the trench, because the epicenter of a historical earthquake simply indicates the center of the area of maximum damage (i.e. the center of the "epicentral region"), but the source fault of the 1822 event must be at least 100 km long based on magnitude/length relationships, so it could easily go through the trench site and have an epicenter elsewhere to the north. In fact, the isoseismals (lines of equal seismic intensity) plot for the 1822 event of Ambraseys (1989) shows the maximum intensity as an elongated region trending NNE, where the largest intensity isoseismal contains the trench location.

If we consider all the evidence together, the most logical interpretation is that the likely source of the 1872 event was the southernmost tip of the Amanos segment and, given the widespread damage also reported all the way from Antakya to Samandağ, and in the mountain villages on the Amanos mountains aligned parallel to this trend (Ambraseys, 1989), the faulting likely extended in that direction towards the coast, possibly by linking with faults in the Antakya fault zone (Figure 2b). Ambraseys (1989) plots isoseismals aligned with the southern termination of the Amanos segment and centered on the Hatay graben. Ambraseys & Jackson (1998) stand by the earlier interpretation of ground rupture for the 1872 event, as they report a 20 km rupture length for this event in their catalog of "surface rupturing earthquakes". This leaves the 1822 earthquake as the only possible rupture in the 1801–1940 age range to go through the trenches at Demirköprü, because it is very unlikely that an unknown ground-rupturing earthquake (i.e. a large one) would be missing from the records after 1800, especially one that would have strongly affected such a historically important river crossing as the one at Demirköprü. If this is the case, then also the event of compatible age ("after 1650 AD") found by Akyüz et al. (2006) in the next trench further south (Ziyaret, Figure 3) should be the 1822 earthquake.

The 1822 earthquake was a large event, as shown also by the fact that it was followed by 1.5 years of rather large aftershocks (Ambraseys, 1989, 2009), with the full aftershock sequence terminating only after 30 months (Salamon, 2008). Ambraseys (1989) and

Ambraseys & Jackson (1998) estimated a magnitude of 7.5, which seems reasonable given the large area it affected and the level of damage reported everywhere. Without explaining why, Sbeinati et al. (2005), though also describing this as one of the most damaging earthquakes in the region, reduced the magnitude to 7.0. A clue to the magnitude change could be the fact that several localities in Turkey that had reported considerable damage (e.g. Gaziantep, and the towns west and northwest of it) are not listed in their catalog, which would reduce the size of the affected area and thus the magnitude. As there is no reason for the omission of these localities, we accept the determination of M_w 7.5 of Ambraseys & Jackson (1998).

Different authors have placed the 1822 event either on the Amanos fault (e.g. Seyrek et al., 2007), the Yesemek fault (e.g. Ambraseys & Melville, 1995; Duman & Emre, 2013), or the St. Simeon fault (e.g. Karakhanian et al., 2008; Darawcheh et al., 2022). Even not considering the likely presence of this earthquake in the trenches of Altunel et al. (2009) and Akyüz et al. (2006) along the Orontes river valley, the Amanos fault is the least likely option: (1) the damage pattern from the 1822 M_w 7.5 earthquake is shifted east and south compared to the damage pattern of the 2023 M_w 7.8 earthquake (which definitely ruptured the Amanos segment, see Figure 2b), (2) several foreshocks (the strongest preceding the mainshock by 30 minutes) occurred in the region between Antakya, Latakia and Aleppo (Ambraseys, 1989, 2006), suggesting that the main shock may have been triggered by the rupture of one of the many N-S faults between the northern Ghab basin and the Amik basin, and (3) the epicenter estimated for the 1822 event by both Ambraseys (1989) and Sbeinati et al. (2005) is located ~20 km east of the Yesemek fault trace, albeit 60 km apart in latitude in either work (the location shift is also likely due to the exclusion of the Turkish area around Gaziantep from the 2005 catalog). In addition, Duman & Emre (2013) found no signs of a recent rupture along the Amanos fault in the Karasu valley, whereas they claim that the Yesemek fault appears to show a fresher morphology, at least in its northern segment (which is the one they checked in the field, on the Turkish side of the border). Ambraseys (1989) identified the maximum intensity isoseismal as approximately parallel to and slightly west of the Gaziantep-Kilis-Idlib trend. This is consistent with the position and orientation of both the Yesemek fault and the northern segment of the St. Simeon fault. Darawcheh et al. (2022) explicitly argue for the 1822 event to have originated on the St. Simeon fault. These authors, however, identify as source fault what they call the “middle segment” of the St. Simeon fault (actually, it is the southern segment, see Figure 4): this is a mere 26 km long and a series of

very short en-echelon segments (possibly a shear zone without a throughgoing fault near the surface), i.e. too short to produce an earthquake of this magnitude. Considering the parameters quoted by these authors (M_w 7.3 and a fault width of 15 km), an average fault slip of about 10 m would be required, which is unrealistically large, as this is the typical average slip value for M_w 8.0 (Wells & Coppersmith, 1994). A 26 km long fault would normally produce roughly a M_w 6.7 earthquake, which does not match at all the historical descriptions of destruction spread over a vast region. For the St. Simeon fault to be the source of the 1822 earthquake, it would have had to rupture all the way from Afrin in the north to Sahen in the south (i.e. rupturing part of the Apamea fault as well), breaking across the southern segment too, which has a trend ~30˚ off from that of the two adjacent faults and, as pointed out above, appears to be more a broad shear zone than a throughgoing fault. Also, if a surface rupture had extended to the northeastern Ghab basin, the intensity at Maarret Missrin, Ram Hamdan, and Binnish (all between 6 and 12 km from the southern St. Simeon fault segment) should have been above the VII reported in Sbeinati et al. (2005). Finally, Karakhanian et al. (2008), while speculating that the 1822 event may have occurred on the northern segment of the St. Simeon fault (based on the epicenter location of Sbeinati et al., 2005), found no evidence of a recent surface rupture on it, including at the site of the St. Simeon monastery, which they studied extensively.

The most likely candidate for the 1822 earthquake thus appears to be the Yesemek fault combined with part of the Qanaya-Babatorun fault, with a rupture extending from the Yesemek fault northern segment for ~100–120 km south, past the Demirköprü bridge, to at least the Ziyaret trench of Akyüz et al. (2006) (Figure 2b, 3). The next trench south (Yazlık) does not have an event of compatible age, though it is possible that the event is simply not visible in the trench because it followed a slightly different strand. In any case, a rupture from the latitude of Islahiye in the north to south past Demirköprü and into the Orontes valley would explain the especially strong damage in the Quseir region (which was also struck by numerous aftershocks, reported by Ambraseys, 2009) and at the main crossings on the Orontes river (Demirköprü and Jesr Al-Shughour), and the high damage region extending all the way to Sagce and Gaziantep in the north.

The Yesemek fault has usually been mapped continuing south to the eastern edge of the Amik basin (Duman & Emre, 2013) and possibly connecting to the Armanaz fault (Seyrek et al., 2014). The Yesemek fault, however, splits into two branches south of 36.616643°N, both of which are mapped as “active faults” in the active faults database of

Zelenin et al. (2022). One branch (the one called "Yesemek fault" or "East Hatay fault" by previous authors, see Appendix B) continues with an almost N-S trend, whereas the other one turns southwest, following a series of low hills, then disappears under the sediments of the Amik basin (Figure 2). We also know that there is an active fault in the middle of the Amik basin. This fault is visible in the seismic line of Perinçek & Çemen, 1990, and was re-interpreted by Seyrek et al. (2014), who reviewed and synthesized existing subsurface data. Old geographic maps also show that the eastern shoreline of the former Lake Amik and the eastern limit of the swamps north of the lake followed this buried fault closely all the way to the eastern edge of the Karasu valley, meeting the Yesemek fault there. It seems likely that this is the source fault of the 1822 earthquake (Figure 2b), and that the fault interpreted by previous authors below the Amik basin is in fact the Yesemek fault, which continues south and connects to the Qanaya-Babatorun fault near Demirköprü.

The next pair of events that should be examined together is that of 1408 and 1404. The 1408 event has been identified most likely in all three trenches of Akyüz et al. (2006), who dated event E1 "between 1310 and 1423" in the northernmost trench and "younger than 1019" in the southernmost one. It could of course be either the 1404 or the 1408 earthquake, but as we will see the 1404 earthquake is unlikely to have ruptured this far north. The maximum destruction from the 1408 earthquake was along the trend from the Quseir region to Jesr Al-Shughour, with significant damage also to Mahalibeh castle, and damage to Jableh and Latakia along the coast. There is an open argument about the reported surface rupture, depending on the interpretation of the Arabic word for the distance, given as either ~20 km (Ambraseys, 1989, 2009) or ~2 km (Guidoboni & Comastri, 2005). The latter also claim there is no proof of damage in Antakya (which in their case means magnitude reduction from the 6–7 of Ambraseys & Jackson, 1998, to ~5.5), but Ambraseys (2009) reiterates that damage in Antakya is confirmed in reliable near-contemporary Ottoman calendar sources, which Guidoboni & Comastri (2005) do not seem to be aware of, as they do not mention them. Ambraseys (1989) puts forward two possibilities for the source fault: either the Qanaya-Babatorun fault, or the Antakya fault zone, the latter based on the fact that the damage extends towards the SW to the coast. A matter of contention here is again the presumed surface rupture described in historical sources. Regardless of its length, the location of the rupture is debated, because there is no agreement on where the village mentioned in the ancient texts is located, near which the rupture may have terminated (the starting point was in the Quseir region, i.e. between Antakya and the Orontes gorge, so not

very specific either). There are multiple spellings reported (Salthuam, Shalfuham, Salfhoum, Salthum), and this place is identified by Ambraseys (1989, 2009) as Hisn Tell Kashfahan (in Jesr Al-Shughour), and by Sbeinati et al. (2005) as Sfuhen (Sufuhon, on the eastern shoulder of the Ghab basin, Figure 1). The latter seems to be too far east, and located on faults that are not connected to anything in the Orontes gorge, but it could have been affected by a landslide triggered by the earthquake. So, if Sufuhon is indeed the location mentioned, a landslide and a fault surface rupture must have occurred at two different places. If Hisn Tell Kashfahan is the correct interpretation, then landslide and fault surface rupture could have been at the same place. Either way, the earthquake seems to have particularly affected one location that is clearly identifiable: the twin fortresses of Shugr and Bekas (Shugur Qadim), located less than 2 km west of the Qanaya-Babatorun fault. The key crossing on the Orontes of Jesr Al-Shughour, which sits on this fault trace, was also destroyed. In Antakya, however, the damage does not appear to have been as extensive, so the Qanaya-Babatorun fault seems a far more likely candidate than the Antakya fault zone, even without considering the information from the trenches. The fault rupture most likely did not extend north past the northernmost trench of Akyüz et al. (2006), because otherwise we would expect reports of destruction at the Demirköprü historical "iron bridge", as this crossing was a vital one that had been in existence since well before 1000 AD. A ~40 km long rupture starting at about the northern trench site and extending to Jesr Al-Shughour would produce a M_w 7.0 earthquake, in line with Ambraseys & Jackson (1998) estimate of a "6 to 7" magnitude. A 20 km long rupture limited to the northern part of the fault appears too short to account for the significant damage extending all the way to Mahalibeh castle, and a 2 km long rupture is unrealistic, as the corresponding M_w 5.5. event would be too small to cause any damage along the coast in Latakia and Jableh, which are 70 to 80 km away.

There is less information for the 1404 earthquake: Ambraseys (2009) and Guidoboni & Comastri (2005) give essentially the same description from the same primary sources, and both point out that one source wrongly adds some 1408 localities to the 1404 event description. Sbeinati et al. (2005) used this source instead, apparently not realizing the problem, and estimated M_w 7.4. Ambraseys & Barazangi (1989) estimated $M_w \geq 7.0$. This means the surface rupture of the 1404 earthquake must have been at least 40 km long. From the damage distribution, the source fault has to be somewhere around the Ghab basin. The Qanaya-Babatorun fault is too far north to account for the significant damage to Marqab castle (on the coast, 25 km south of Jableh), and for the intensity VII–VIII reported from

Tripoli in Lebanon. The Missyaf segment to the south is not a likely source, because the last event on this segment, visible in the trench and in the displaced Roman aqueduct at Al-Harif, is the 1170 earthquake (Meghraoui et al., 2003; Sbeinati et al., 2010). The two likely sources left are the Nusayriyah fault at the western margin of the Ghab basin, and the Apamea fault at its eastern margin (Figure 2a). We believe the Nusayriyah fault to be the more likely source, based on two considerations. The first is that the high damage reports are skewed towards the coast, pointing to a source on the western rather than eastern Ghab basin, and the second is that an earthquake on this fault segment in 1404 would be more effective in increasing the stress on the Qanaya-Babatorun fault, which ruptured just 4 years later, than an earthquake on the Apamea fault. A final possibility, which we cannot discount at this time, is that the earthquake resulted from the rupture of a fault buried in the middle of the Ghab basin, as the presence of a fault here is known from geophysical data (Rukieh et al., 2005).

The next significant event back in time in this area is the 1170 earthquake, which is well-documented, with extensive descriptions by multiple authors (e.g. Ambraseys 1989, 2004, 2009; Guidoboni et al. 2004b; Guidoboni & Comastri 2005). Guidoboni et al. (2004b) estimated M_w 7.7 +/- 0.22 and a fault length of 125 km. Ambraseys (2009) instead estimated M_w 7.3 +/- 0.3. The source fault of this earthquakes has been identified by Meghraoui et al. (2003) as the Missyaf segment of the DSF, with the 1170 event being the last rupture that occurred at the Al-Harif aqueduct site. They suggested that the fault ruptured from Qalaat El Hosn to Apamea, a distance of ~80 km. Meghraoui et al. (2003) and Sbeinati et al. (2010) established that the slip at the aqueduct site in the 1170 event was 4 to 4.5 m. If this is maximum slip, it alone indicates M_w 7.3 to 7.4. This is compatible with the magnitude estimate of Ambraseys (2009), and reasonably compatible with the damage distribution. The only outlier is the city of Aleppo as reported by Guidoboni et al. (2004b), but Sbeinati et al. (2010) argue that these authors overestimated the damage in Aleppo based on an erroneous interpretation of the chronicle by Ibn Al Athir. The argument of Sbeinati et al. (2010) is reasonable, because the damage distribution is otherwise very unusual, with a single intensity X locality (city of Aleppo) isolated and 200 km away from the main intensity X region (Lebanon-Syria border southwest of Qalaat El Hosn). We therefore agree with the source fault identification and rupture length of Meghraoui et al. (2003) and Sbeinati et al. (2010).

In 1156–1157 there was a long earthquake sequence (an “earthquake storm”) in the region between Homs and Aleppo, culminating with the largest event on Aug. 12, 1157 (Ambraseys, 2004, 2009). Guidoboni et al. (2004a) did not calculate magnitude or epicentral

area because of the difficulty in separating the numerous earthquakes in this period. Ambraseys (2004, 2009) instead separated several of the larger events and calculated the magnitude of the largest (7.2 +/- 0.3), and placed the location of the epicenter very close to the Missyaf fault near Apamea. As mentioned above, the Missyaf fault last ruptured in 1170 through the Al-Harif site. While it is possible that an older rupture followed a slightly different strand and did not pass through the Al-Harif site, the Coulomb stress shadow due to an earthquake in 1157 would have most likely precluded another large rupture of the same fault segment just 13 years later, because such a short time is insufficient to significantly reduce the coseismic stress shadow from a $M_w > 7$ event. Based on the damage pattern, the St. Simeon fault is too far north, and the Nusayriyah fault too far west. That leaves the Apamea fault and another unnamed fault of similar length just 10 km east of it (which here we name "Shaizar fault", Figure 2a, 4). Because it appears that the most damage was towards southeast (Hama, Salamiyah) and east (Ma'arat al-Nu'man, Kafar Tab, Shaizar) of the Ghab basin, the Shaizar fault is a more likely source than the Apamea fault. Sbeinati et al. (2005) put the epicenter on the Shaizar fault. Also, all of the 1156-1157 seismicity was concentrated in the region between Aleppo and Hama east of this fault. The area is littered with small faults (Figure 4), so it is conceivable that this is a case of small and moderate earthquakes triggering one another, until one of them got close enough to trigger the largest of these faults to rupture. The Apamea fault cannot, however, be excluded as a possible source without further investigation.

We have previously argued that the St. Simeon fault is unlikely to be the source of the 1822 earthquake. There are two older earthquakes, however, which could have been produced by this fault, in 1626 and 1138. The interpretation of this fault is controversial: some authors (e.g. Westaway, 2004; Seyrek et al. 2014) claim that it belongs to an earlier tectonic phase and it is no longer active. Others (Rukieh et al., 2005) instead consider it active, and some (Karakhanian et al., 2008) have even found evidence of historical earthquake-related deformation along it, albeit not an actual rupture of the main fault itself.

There is little information about the 1626 earthquake. Ambraseys only mentions it in his 2009 catalog and in Ambraseys & Finkel (1995), and Sbeinati et al. (2005) repeat the same information, add one paragraph, and estimate a magnitude of 7.3. It appears to have been a fairly damaging earthquake over a large area, but not much specific information has come to light. Karakhanian et al. (2008) consider the St. Simeon fault a likely source, based on their archeoseismological work on the St. Simeon monastery. A rupture of the northern

segment of the St. Simeon fault (~ 50 km long) could produce a M_w 7.2 earthquake, and in light of the reported damage area (between Aleppo and Gaziantep) we believe that this fault is indeed a likely candidate.

The authors who report extensively on the 1138 event are Ambraseys (2004, 2009), Guidoboni et al. (2004a), and Guidoboni & Comastri (2005). Sbeinati et al. (2005) just give it a brief mention, and this event does not even appear in the GEM historical catalog of Albini et al. (2013). An estimated magnitude is only reported by Guidoboni & Comastri (2005) (M_e 6.0), and apparently recalculated (without explanation, but from comparing the reported intensities it seems it was done by just increasing the estimated intensity values) in the INGV catalog to M_e 7.5 (Guidoboni et al., 2018, 2019). Both Ambraseys (2004, 2009) and Guidoboni & Comastri (2005) essentially give the same description concerning localities and damage, and date of the earthquake. Guidoboni & Comastri (2005) also calculate the position of the epicenter on Mount Quros, which is just 15 km north of the termination of the St. Simeon fault. On the basis of where the highest damage was, and where the earthquake was felt, the St. Simeon northern straight segment, which could produce a M_w 7.2 earthquake, is a likely source. The estimated M_e 7.5 (INGV) is excessive, because it corresponds to a 110-120 km long rupture, which would mean a rupture involving also the Apamea fault into the northern Ghab basin, with a very different damage distribution. In fact, Guidoboni et al. (2014a) suggested that the entire 1138-1139 sequence involved faults north-northeast of the Ghab basin, and not any of the faults that bound the basin itself. Besides the northern St. Simeon fault, there are no other long enough faults in the vicinity and in the proper position that would give the observed damage pattern. A magnitude of 6.0 (Guidoboni & Comastri, 2005) on the other hand is too small, because such an earthquake would have a radius with strong (VI) shaking of only about 20 – 30 km, and several localities that reported significant damage (e.g. Tell Khalid, Tell Amar, Bizaah) are 60 to 100 km away.

2.1.2 Karasu valley and East Anatolian fault zone

The pairing of earthquakes and source faults along the EAF north of the Karasu valley, between Türkoğlü and Elâziğ, is somewhat more straightforward - albeit not entirely free of controversy - because there are fewer active faults that need to be considered, and fewer post-AD 1000 large earthquakes. We have included one earthquake from 2020 with M_w 6.8 (Elâziğ earthquake, Table 2), which is below our M_w 7.0 limit, because this is the

449 only instrumental, 21st century and pre-2023 earthquake to have occurred along the EAF and
450 it delimits the 2023 M_w 7.8 rupture northeastern extent (Figure 2b), so it is included here for
451 completeness. This earthquake ruptured part of the Pütürge segment and did not appear to
452 have a surface rupture (Çetin et al., 2020), though ~0.5 m of shallow slip was identified by
453 Pousse-Beltran et al. (2020).

454 The 2020 Elâziğ earthquake rupture is sandwiched between two other relatively
455 recent events: 1874 M_w 7.1 and 1893 M_w 7.2 +/- 0.1 (Ambraseys, 1989; Ambraseys &
456 Jackson, 1998; Ambraseys, 2009). Ambraseys (2009) reported that he confirmed in the field
457 in 1967 the surface rupture of the 1874 event, which involved the Palu segment between Palu
458 and Pütürge (Ambraseys & Melville, 1995). His evaluation of the historical documents
459 indicates a ground rupture about 45 km long, with 1–2 m uplift of the eastern block and
460 unspecified left-lateral strike-slip displacement.

461 The 1893 calculated epicenter (Ambraseys, 2009) is near Çelikhan, and Ambraseys &
462 Melville (1995) attributed the earthquake to the Erkenek segment. In the historical reports a
463 surface rupture is not described anywhere, but for an earthquake of this magnitude it would
464 be in the range of 45 to 70 km long. The rupture did not propagate south into the Pazarcık
465 segment, as there is no trace of it in the Balkar and Tevekkelli trenches (Figure 3) of Yönlü
466 (2012). On the basis of the isoseismal plot and epicenter location of Ambraseys (2009), the
467 earthquake likely ruptured most of the Erkenek segment, stopping ~ 20 km SW of Pütürge in
468 the north, and near Erkenek in the south (Figure 2b). A smaller (M_w 6.8) event in 1905 with a
469 similar epicentral area may have completed the rupture of this fault segment to the south,
470 likely without a surface rupture (it does not appear in the "surface rupturing" event list of
471 Ambraseys & Jackson, 1998, whereas the 1893 event does).

472 The last rupture of the Pazarcık segment prior to 2023 is well-documented, because
473 multiple trenches have been excavated across it (Yönlü, 2012). There are two historical large
474 events in the vicinity of this segment that we need to consider: one in 1114, and the other in
475 1513/1514. The oldest of the two is the better documented one, even though it appears as two
476 separate events in different catalogs. This earthquake is discussed in detail by Ambraseys
477 (2004), who reported it as having happened on Nov. 29th 1114. Ambraseys (2004, 2009) went
478 to some length to explain why there are differences in reported dates, and concluded that
479 Nov. 29th 1114 is the correct one. This earthquake was assigned a magnitude of "large" (i.e.
480 7.0 to 7.8) by Ambraseys & Jackson (1998), and 6.9 +/- 0.3 by Ambraseys (2009). Guidoboni
481 & Comastri (2005) instead split the event in two, on different dates and locations (Nov. 13th

1114 Maraş, M_e 6.3, and Nov. 29^h 1115 Misis, M_e 6.4). Ambraseys (2009) states that it is unclear why they split the event and that in 1114 there were several other strong shocks in the region before the one on Nov. 29th, but the latter was by far the largest one in the series. One of the two shocks of Guidoboni & Comastri (2005) (Nov. 13th 1114) is in fact listed as a separate foreshock by Ambraseys (2009). Ambraseys (2009) also reported that some sources mention an earthquake in this region in 1115, and this was likely a strong aftershock. Sbeinati et al. (2005) also split the earthquake into two events that have same description and same general area, but different magnitudes (7.4 and 7.7), both of them in Nov. 1114 (no day given, they just state within the same entry that this event could be two earthquakes). Here the confusion is increased by the fact that in the parametric list the authors supply two distinct epicenters and magnitudes, but an identical list of affected localities and intensities, so it is unclear how they were able to compute different epicenters and magnitudes. One of the two (M_w 7.4, with epicenter near Şanlurfa, east of the Euphrates valley) has been included in the GEM catalog of Albini et al. (2013), whereas the second 1114 earthquake in the GEM catalog has been taken from Ambraseys (2009), again a choice without apparent explanation. There is no trace in Ambraseys's papers and in his 2009 catalog of any events in 1114 that affected mainly the region around Şanlurfa: the two significant "foreshocks" mentioned were in the Iskenderun bay region. In fact even the 1115 event of Guidoboni & Comastri (2005) is located between the Iskenderun bay region and Maraş. Ambraseys (2009) stressed how the descriptions of this earthquake are split between "western" and "eastern" primary sources: this could explain the tendency of recent authors to produce two main shocks for the same event. Finally, the parametric catalog of Kondorskaya & Ulomov (1999) lists for this event M_w 8.1, and the event epicenter location (a single one for 1114, but on August 10, the date for which Ambraseys 2004 reports a strong shock possibly offshore Iskenderun) is placed between the locations of Ambraseys (2004) and Sbeinati et al. (2005). Considering that M_w 8.1 is close to the magnitude expected for a complete rupture of the entire EAF, this catalog clearly overestimates the size. In summary, for the earthquake of November 1114 the works of Ambraseys are more reliable, because there is a justification for each determination made (date, location, magnitude) and clear exclusion of other possibilities. We therefore chose to accept the information given in the latest work (Ambraseys, 2009) for the parameters of this earthquake, which place it somewhere along the Pazarcık segment of the EAF. Yönlü (2012) found a rupture compatible with a 1114 event in three trenches along the EAF (Nacar, and Balkar 1 and 2, Figure 3): there E1 has been dated to before 1153 and after 677, and this rupture is not present in their Tevekkelli trench, 35 km further southwest along the fault.

From the paleoseismological findings a surface rupture length of 60 km has been estimated (Gürboğa, & Gökçe, 2019), placing the 1114 earthquake on the northern two-thirds of the Pazarcık segment with M_w of at least 7.1. This is compatible with the size estimated by Ambraseys (2009), but not with the estimates of Guidoboni & Comastri (2005), Sbeinati et al. (2005), and Kondorskaya & Ulomov (1999), further confirming that the earthquake location of Ambraseys (2009) is most likely the correct one. This event does not appear in any form in the trenches and core from Lake Hazar (Hazar Gölu, Figure 3; Çetin et al., 2003; Hubert-Ferrari et al., 2020), so probably its magnitude was not larger than the estimated 7.1, even though Ambraseys & Jackson (1998) considered it a possible candidate for a truly large earthquake (i.e. of magnitude closer to 7.8 than to 7.0).

The only authors to report on the 1513 earthquake in recent papers and catalogs are Ambraseys (1989, 2009), and Ambraseys & Finkel (1995). The exact year (late 1513 or early 1514) is also debatable. There is very little specific information about the earthquake, but Ambraseys (1989) claims that, given the size of the area over which it was felt (even in the absence of specific damage descriptions), the magnitude was significant ($\geq$ 7.4). Apparently, the regions of Tarsus, Adana, Malatya, and around Haçin were strongly affected. His calculated epicenter location puts the earthquake within 30 km of the EAF (~ 30 km ENE of Türkoğlu), while the uncertainty radius is ~50 km, so a location of the event on the EAF is entirely plausible. The Tevekkelli trench of Yönlü (2012) contains a rupture for E1 dated to between 1440 and 1630, which is compatible with an earthquake in 1513/1514. In the three trenches further northeast along the EAF (Nacar, and Balkar 1 and 2) instead E1 is dated to between 677 and 1153, so the 1513 event is not visible. The closest trench to Tevekkelli (the Nacar trench) is 35 km northeast of it, so the rupture should have stopped before reaching this point, which means it is unlikely for the 1513 earthquake to be the penultimate event (E2) tentatively identified by Çetin et. (2003) in one of their Lake Hazar trenches (they date E2 to AD 1393 – 1464, but claim that, because of dating uncertainties, it could be the 1513 earthquake). In the catalog of trenches in Turkey (Gürboğa & Gökçe, 2019), the 1513 rupture is estimated as 40 km long. This is barely the equivalent of a rupture of the Pazarcık segment between about 10 km southwest of the Nacar trench and Türkoğlu. A 40 km rupture however would not produce an earthquake above M_w 7.0. A M_w 7.4 earthquake requires a 80 km long rupture. That can be done by the rupture extending from south of the Nacar trench to Islahiye, i.e. rupturing the southern part of the Pazarcık segment and then the Nurdağı segment of the Amanos fault to the next bend south near Islahiye (Figure 2b). This would be more in line

549 with an event that must have produced considerable damage to the region of Adana and
550 Tarsus. A rupture stopping at Türkoğlu and a M_w of 7 would not have been sufficient, this
551 region being 180 km away.

552

553 **3 Discussion: timing, location, and size of the 2023 M_w 7.8 Pazarcık earthquake**

554 3.1 Fault segmentation, rupture length, and earthquake size

555 In the Karasu valley, the central and southern Amanos fault (Hassa segment and most
556 of the Kirikhan segment, Figure 2a) does not appear to have ruptured in a large earthquake at
557 any time from at least AD 1000 to 2023 between Baghras and Islahiye, a fault length of ~70
558 km (Figure 2b, 5a). This could partly explain the unusually large size of the 2023 M_w 7.8
559 earthquake: the central and southern Amanos segments, which are separated from the
560 Nurdağı segment by a releasing bend near Islahiye, and from each other by a restraining bend
561 near Demrek (Duman & Emre, 2013), were stressed enough that the bends not only were
562 insufficient to stop a multi-segment rupture but may have contributed to it. In fact, it appears
563 that the Demrek restraining bend was a region of higher slip from the surface to ~10 km
564 depth (Barbot et al., 2003). Recent studies on large thrust earthquakes (e.g. 2008 M_w 7.9
565 Wenchuan earthquake, Wan et al. 2017) suggest that stepovers along faults, and especially
566 restraining stepovers, build up slip deficit over time merely because of their geometric
567 complexity, and when they finally rupture they provide energy for the rupture to propagate
568 even further, which it seems is what happened on the Amanos fault. Thus, the most likely
569 reason we have not seen such large ruptures before on the EAF is not because "fault
570 segmentation" or "fault maturity" determine the maximum length of rupture in plate
571 boundary faults, but rather because they are infrequent and, therefore, not captured by the
572 comparatively short and incomplete earthquake history we have for the region. For a M_w 7.8
573 earthquake to happen, which, let's not forget, ruptured over half of the EAF at once, we need
574 a rather specific set of circumstances that are hard to quantify in the absence of data.

575 Prior to 2023, there was considerable disagreement over the maximum size of
576 earthquakes on the EAF. For example, Hubert-Ferrari et al. (2020), on the basis of the
577 historical seismicity reports, assumed that magnitude 7.0 and above is likely, whereas some
578 studies based on the instrumental record alone considered M_{max} for the EAF to be limited to
579 M_w 6.8 (e.g. Bayrak et al., 2015), while yet others proposed a range from M_w 6.7 to 7.4
580 depending on the segment considered (e.g. Gülerce et al. 2017; Güvercin et al., 2022), with

up to M_w 7.7 when some segment combinations are explored in models (Gülerce et al., 2017). A good estimate of M_{max}, however, is crucial for seismic hazard assessments. In the case of faults like the EAF, which have no large instrumentally-recorded events, knowledge about M_{max}, recurrence intervals, and rupture length can only come from a combination of historical records, paleoseismological studies, geological analysis in tectonic context, and comparisons with similar faults. Based on the information available at the time, the 2023 M_w 7.8 earthquake could have been foreseen in terms of location and timing (an earthquake on the southern EAF was due any time, this fault being a clearly active one currently in -what should have been an alarmingly- quiescent period), but not in size, because the largest confirmed earthquake in historical catalogs since AD 1000 for the region reached M_w 7.5 at most, with the majority of earthquakes being M_w 7 to 7.2 (Table 2). Besides, the source fault of the M_w 7.5 earthquake in 1822 is not technically even part of the EAF system. Looking further back in time (before AD 1000) would not have increased the number of truly large earthquakes, as such events are even harder to interpret the older the records are: there are none listed for this area by Ambraseys & Jackson (1998), but that does not mean none happened, just that they may not have been recognized or recorded. With no earthquakes of comparable size in either instrumental or historic catalogs, we cannot calculate an observed recurrence interval for $M_w \geq 7.8$ on the EAF, and are left with estimates based on geodetic rates or longer-term average geological displacement rates (e.g. Friedrich et al., 2003). This is only half the problem though: without a $M_w \geq 7.8$ in the records, the possibility that such an earthquake would occur on the EAF was not seriously considered in seismic hazard calculations for the region by most authors. We propose that for the EAF M_{max} is actually ~ 8.2, i.e. a complete rupture from the Karlıova triple junction to the Amik triple junction (Figure 1d), and that all continental strike-slip plate boundary faults should be treated as having the same end-to-end rupture potential**,** unless proven otherwise. In this context, M_{max} is reached in “superevents” that are infrequent and most likely highly non-periodic, especially for non-isolated plate boundary faults such as the EAF-DSF system (contrast with the Alpine Fault, NZ, Berryman et al., 2012) and thus not captured by even such a comparatively long historical record as we have for Anatolia. The 2023 M_w 7.8 earthquake did not reach M_{max} only by a fortuitous combination of circumstances. It appears that the combined effect of the larger stepover between the Erkenek and Pütürge segments and the coseismic Coulomb stress shadow from the 2020 Elâziğ event on the latter was enough to stop the 2023 rupture from dynamically propagating further to the northeast. Understanding how and in what measure fault geometry and prior stress history each contributed to stopping the rupture will need

615 careful modeling. The 2023 M_w 7.8 earthquake stands as a warning that continental
616 transforms can fully rupture just as subduction thrusts can (see McCaffrey, 2008), in
617 infrequent but devastating earthquakes.

618

619 3.2 Fault interactions, cascades, cycles, supercycles, and collective memory

620 The reason for the behavior of the EAF is multifaceted. First of all, there is the
621 intertwined kinematics of the three plate boundary fault systems: EAF, DSF, and NAF
622 (Figure 1d). Hubert-Ferrari et al. (2003) pointed out that the EAF and NAF cannot move
623 simultaneously, and that in the historical records since AD 100 the number of damaging
624 earthquakes on each fault reflects this, with peak seismic activity switching from one fault
625 zone to the other every few hundred years. For the DSF, Khair et al. (2000) also observe a
626 switching between activity and quiescence, with quiescent periods of 450–700 years
627 interrupted by active periods of 50–150 years in the past two millennia. These are examples
628 of supercycles (e.g. Philibosian and Meltzner, 2020; Salditch et al., 2020).

629 Whereas plate-boundary-scale kinematics and variations in long-term strain
630 accumulation may control the acceleration and the turning-on-and-off of each fault zone on
631 the million-year to the millennial scale (i.e. supercycles and clusters; see also Friedrich et al.,
632 2003; Bennett et al., 2004, Lefevre et al., 2018), within each period of high activity the
633 seismic behavior is likely controlled by coseismic and postseismic Coulomb stress changes
634 (King et al. 1994). The latter is indicated by the clustering of earthquakes within relatively
635 short time periods, and by the propagation of ruptures in systematic fashion along some
636 faults: for example, the classic NAF behavior of east-to-west sequential ruptures (e.g. Barka,
637 1996; Stein et al., 1997; Hubert-Ferrari et al., 2000, 2003), but also the behavior observed on
638 the EAF, where a series of ruptures can start at both ends of the fault system and move
639 towards the center (Hubert-Ferrari et al., 2003). Another potential example of this behavior is
640 the rupture cascade (Philibosian and Meltzner 2021) of the 12th century (cf. Figure 7.2 in
641 Marco and Klinger, 2014) along the EAF and DSF systems in a southerly direction. The 1114
642 event occurred along the Parzarcık segment of the EAF (Figure 2b). Then, the DSF ruptured
643 several times as documented by the 1138, 1157, and 1170 events (Figure 2b and 5), and the
644 1202 event in Lebanon (South Yammouneh segment, DSF, Daëron et al., 2007). After the
645 12th century cascade, both fault zones appear to have ruptured irregularly. As a result, the
646 time since the last major ($M_w > 7$) event varies along strike of the fault zones. For the EAF,

the times since the last rupture events are130 years (Erkenek segment), 500 years, 900 years, and over 1000 years for the Amanos segment (Figure 5a). These seismic gaps are not due to a lack of data, but rather are an expression of the natural earthquake behavior in active fault zones. Thus, for fault segments where a seismic gap exists, the maximum possible earthquake magnitude (M_{max}) may be severely underestimated unless seismic activity from the entire fault system going back several thousand years is considered. For example, seismic hazard modeling conducted solely based on instrumental seismic records prior to February 6th, 2023, treated such segments as inactive and underestimated M_{max} and the seismic hazard (e.g. Bayrak et al., 2015). The February 6th, 2023 Pazarcık earthquake filled in the large seismic gaps in the Amanos segment and several other seismic gaps along strike (Figure 5b). If the same type of hazard modeling would be conducted after February 6th, the Amanos segment will appear as active and be included, thereby likely overestimating its hazards in the near future.

Similar seismic gaps also exist along the DSF, some lasting for 200 years, while others lasting for 620 years, and over 850 years (Figure 5c). These seismic gaps will grow, close, and reopen repeatedly (Figure 5d) as long as strain accumulates across this active plate boundary, and when a seismic gap exists without a recent stress shadow, the hazard is high. The identification of seismically inactive but geodetically active regions along active fault zones is, therefore, an important area of focus for future research and seismic hazard assessment, but additional information is required to accurately forecast earthquake potential.

There is also an important role played by local fault configuration, in this case especially the branching of EAF and DSF. The two systems are not independent, even on short time scales. These two fault zones overlap, with faults from both zones running parallel to one another and having very similar kinematics in a strip just a few tens of km wide. Thus, in the Karasu valley and Amik basin, depending on exactly which fault ruptures where, there can be either Coulomb stress loading or shadowing of neighboring faults belonging to either fault zone. For example, the northwestern DSF strands (Qanaya-Babatorun and Nusayriyah faults) have likely been loaded coseismically by the 2023 M_w 7.8 earthquake, simply on the basis of their relative position, geometry, and kinematics. On the other hand, the Amanos segment and the Yesemek fault in the Karasu valley have the same configuration as the southern San Andreas/San Jacinto fault pair in California: two closely-spaced (15 to 30 km) subparallel faults with the same strike-slip kinematics. This is a situation where the faults are effectively coupled: a large rupture on one fault would cause a significant coseismic

Coulomb stress drop on the other, delaying the next rupture (Carena et al., 2004). The 1822 earthquake on the Yesemek fault therefore must have delayed the occurrence of the next earthquake on the central-southern Amanos fault, which at that point had not seen a rupture for at least 800 years, and the end of this delay just happened to coincide with a fortuitous rupture propagation from a minor fault in the Narlı fault zone (Figure 2a) to the main branch of the EAF (Rosakis et al., 2023; U.S. Geological Survey, 2023), at a position on the Pazarcık segment of the EAF that also had not seen a rupture in 900 years. This was a classic "domino effect" with all tiles in the right place at the right time. We are thus left with a question that can be answered only with further investigations: how often can the tiles line up in this specific order? It is not a trivial problem: not only a specific set of circumstances can lead to an unusually large event, but also activity on one fault system could control the timing of the next supercycle of its immediate neighbor. It means that calculation of earthquake probability cannot be restricted to one fault, or even one fault system: in the case of continental plate boundary faults, it also needs to include the neighboring fault systems. Plate boundary faults may not just have a "long term memory" (Salditch et al., 2020), but also a "collective memory" due to their coupling by geometric characteristics of the fault systems and stress transfer patterns between them, which would call for earthquake probability calculation at much larger scales than is generally considered.

4 Conclusions

Within the limitations of the information available, we were able to define the most likely pairs of historical earthquakes and their source fault segments along the EAF and northern DSF since AD 1000. We tried to provide a comprehensive explanation for the choices we made in each case, so that the data we produced can be evaluated for level of uncertainty, and used by others either for earthquake modeling, or to identify locations that should be targeted in future paleoseismological studies.

By considering the previous rupture history and geometric configuration of the faults involved, we were able to address the reasons why the 2023 M_w 7.8 earthquake occurred on the southern half of the EAF, why the conditions were right for it to occur now, and why it was unusually large compared to previous events in the region. The main branch of the EAF had a seismic gap of at least 1000 years at its southern end. A major rupture here was likely delayed by the 1822 earthquake on the Yesemek fault (which could explain why the 1872

rupture did not propagate northwards), but the stress shadow from this dissipated in about a century, paving the way for any rupture to either initiate on or propagate unimpeded into the southern Amanos segment. Based on the historical seismic records of the region, the 2023 M_w 7.8 Pazarcık earthquake was foreseeable in space and time, but not in size. M_{max} for the EAF is likely ~ 8.2, with the limit rupture length being the distance between the two triple junctions that delimit it. The 2023 earthquake may not have reached M_{max} simply by a fortuitous combination of factors: if the 2020 Elâziğ earthquake had not happened where and when it did, would the 2023 rupture have continued propagating towards the northeast? This is a question that could be answered by combining Coulomb stress models and dynamic rupture models. If nothing else, what we have learned from the 2023 M_w 7.8 Pazarcık earthquake is that segmentation of continental transform faults is not relevant for calculating M_{max}, because some earthquakes can jump across segment boundaries. Such earthquakes are so infrequent, however, that they are difficult to study, and therefore hard to foresee.

Acknowledgments

We are grateful to Z. Cakir, J. Hubbard, and two other anonymous reviewers for their insightful comments.

Open Research

All the data and software we used have been published or made available by the authors and entities cited in the references list: digital elevation models (Euopean Space Agency, 2021, https://doi.org/10.5270/ESA-c5d3d65 [Dataset], Tozer et al. , 2019, https://doi.org/10.1029/2019EA000658 [Dataset]), active fault database (Zelenin et al. 2022, https://doi.org/10.5194/essd-14-4489–2022 [Dataset]), pixel-tracking data (ForM@Ter – EOST , 2023, doi:10.25577/EWT8-KY06 [Dataset], Ou et al. 2023, https://dx.doi.org/10.5285/df93e92a3adc46b9a5c4bd3a547cd242 [Dataset]), preliminary surface rupture mapping (Reitman et al., 2023, https://doi.org/10.5066/P985I7U2 [Dataset]), and texture-shading program (Brown, 2014; https://app.box.com/v/textureshading [Software]). The file with the electronic version of the ruptures listed in Table 2 and shown in Figure 2b is part of the supplementary material. We have also included in the supplement the uninterpreted base images of Figures 2b and 4.

References

745 Akyüz, H. S., Altunel, E., Karabacak, V., & Yalçiner, Ç., (2006), Historical earthquake
746 activity of the northern part of the Dead Sea Fault Zone, southern Turkey.
747 *Tectonophysics, 426 (1-2)*, 281–293. https://doi.org/10.1016/j.tecto.2006.08.005
748 Albini, P., Musson, R. M. W., Gomez Capera, A. A., Locati, M., Rovida, A., Stucchi, M., &
749 Viganò, D. D., (2013), Global Historical Earthquake Archive and Catalogue (1000-
750 1903), GEM Technical Report 2013-01 V1.0.0, 202pp., GEM Foundation, Pavia,
751 Italy, doi: 10.13117/GEM.GEGD.TR2013.01.
752 Altunel, E., Meghraoui, M., Karabacak, V., Akyüz, S. H., Ferry, M., Yalçiner, Ç., et al.,
753 (2009), Archaeological sites (Tell and Road) offset by the Dead Sea Fault in the Amik
754 Basin, Southern Turkey. *Geophysical Journal International*, *179*, 1313–1329. doi:
755 10.1111/j.1365-246X.2009.04388.x
756 Ambraseys, N.N., (1988), Engineering seismology. *Earthquake Engineering and Structural*
757 *Dynamics 17*, 1–105. https://doi.org/10.1002/eqe.4290170101
758 Ambraseys, N. N., (1989), Temporary seismic quiescence: SE Turkey. *Geophysical Journal*
759 *International, 96(2)*, 311–331. https://doi.org/10.1111/j.1365-246X.1989.tb04453.x
760 Ambraseys, N. N., (2004), The 12th century seismic paroxysm in the Middle East: a historical
761 perspective. *Annals of Geophysics, 47*, 733–758. DOI: 10.4401/ag-3303
762 Ambraseys, N., (2009), Earthquakes in the Mediterranean and the Middle East: A
763 multidisciplinary study of seismicity up to 1900. Cambridge University Press, New
764 York, 947 pp. https://doi.org/10.1017/CBO9781139195430
765 Ambraseys, N. N., & Barazangi, M., (1989), The 1759 earthquake in the Bekaa Valley:
766 Implications for earthquake hazard assessment in the Eastern Mediterranean region.
767 *Journal of Geophysical Research: Solid Earth, 94*, 4007–4013.
768 https://doi.org/10.1029/JB094iB04p04007
769 Ambraseys, N. N., & Finkel, C., (1987), Seismicity of Turkey and neighbouring regions
770 1899-1915. *Annales Geophysicae, Series B, 5(6)*, 701–725.
771 Ambraseys, N. N., & Finkel, C., (1995), The seismicity of Turkey and adjacent areas: A
772 historical review, 1500–1800. Eren, Istanbul, 1995, 240 pp.
773 Ambraseys, N. N. & Jackson, J. A., (1998), Faulting associated with historical and recent
774 earthquakes in the Eastern Mediterranean region. *Geophysical Journal International,*
775 *133*, 390–406. https://doi.org/10.1046/j.1365-246X.1998.00508.x
776 Ambraseys, N. N. & Melville, C. P., (1995), Historical evidence of faulting in Eastern
777 Anatolia and Northern Syria. *Annali di Geofisica, 38*, 337–343. DOI: 10.4401/ag-
778 4110

779 Barbot, S., Luo, H., Wang, T., Hamiel, Y., Piatibratova, O., et al., (2023), Slip distribution of
780 the February 6, 2023 M_w 7.8 and M_w 7.6, Kahramanmaraş, Turkey earthquake
781 sequence in the East Anatolian Fault Zone. *Seismica*, 2.3.
782 doi:10.26443/seismica.v2i3.502
783 Bayrak, E., Yılmaz, Ş., Softa, M., Türker, T., & Bayrak, Y., (2015), Earthquake hazard
784 analysis for East Anatolian fault zone, Turkey. *Natural Hazards*, *76*, 1063–1077.
785 https://doi.org/10.1007/s11069-014-1541-5
786 Bennett, R. A., Friedrich, A. M., & Furlong, K. P., (2004), Codependent histories of the San
787 Andreas and San Jacinto fault zones from inversion of fault displacement rates.
788 *Geology*, *32(11)*, 961–964. https://doi.org/10.1130/G20806.1
789 Barka, A., (1996), Slip distribution along the North Anatolian fault associated with the large
790 earthquakes of the period 1939 to 1967. *Bulletin of the Seismological Society of*
791 *America, 86(5)*, 1238–1254. https://doi.org/10.1785/BSSA0860051238
792 Berryman, K. R., Cochran, U. A., Clark, K. J., Biasi, G. P., Langridge, R. M., & Villamor, P.,
793 (2012), Major earthquakes occur regularly on an isolated plate boundary fault.
794 *Science*, *336*(6089), 1690–1693. DOI: 10.1126/science.1218959
795 Brown, L., (2014), Texture Shading: A New Technique for Depicting Terrain Relief.
796 [Software] 9th ICA Mountain Cartography Workshop, Banff, Canada.
797 https://app.box.com/v/textureshading
798 Carena S., Suppe J., & Kao, H., (2004), Lack of Continuity of the San Andreas Fault in
799 southern California: 3-D fault models and earthquake scenarios. *Journal of*
800 *Geophysical Research: Solid Earth*, *109*, B04313, doi:10.1029/2003JB002643
801 Çetin, H., Güneyli, H., & Mayer, L., (2003), Paleoseismology of the Palu-Lake Hazar
802 Segment of the East Anatolian Fault Zone, Turkey. *Tectonophysics, 374*, 163–197.
803 doi:10.1016/j.tecto.2003.08.003
804 Çetin, K. O., Ilgac, M., Can, G., Çakır, E., & Söylemez, B., (2020), January 24, 2020 Elazığ-
805 Sivrice earthquake (M_w=6.8) reconnaissance study report (METU/EERC 2020-01):
806 Middle East Technical University.
807 Daëron, M., Klinger, Y., Tapponnier, P., Elias, A., Jacques, E. & Sursock, A., (2007),
808 12,000- year-long record of 10 to 13 paleo-earthquakes on the Yammoûneh fault,
809 Levant fault system, Lebanon. *Bulletin of the Seismological Society of America,*
810 *97(3)*, 749–771. doi: 10.1785/0120060106

Darawcheh, R., Abdul-Wahed, M.K., & Hasan, A., (2022), The Great 1822 Aleppo Earthquake: New Historical Sources and Strong Ground Motion Simulation. *Geofisica Internacional, 61(3)*, 201–228.

Duman, T.Y., & Emre, Ö., (2013), The East Anatolian Fault: geometry, segmentation and jog characteristics. In A. H. F. Robertson, O. Parlak, & U. C. Ünlügenç (Eds.), *Geological Development of Anatolia and the Easternmost Mediterranean Region. Geological Society, London, Special Publications, 372*, http://dx.doi.org/10.1144/SP372.14

European Space Agency, Sinergise (2021). Copernicus Global Digital Elevation Model. [Dataset] https://doi.org/10.5270/ESA-c5d3d65. Accessed: 2023-02-12

ForM@Ter – EOST, (2023), Terrain displacement from the Turkiye-Syria earthquakes of February 6, 2023 obtained with the GDM-OPT-ETQ service applied on Sentinel-2 optical imagery. [Dataset] doi:10.25577/EWT8-KY06

Friedrich, A. M., Wernicke, B. P., Niemi, N. A., Bennett, R. A., & Davis, J. L., (2003), Comparison of geodetic and geologic data from the Wasatch region, Utah, and implications for the spectral character of Earth deformation at periods of 10 to 10 million years. *Journal of Geophysical Research: Solid Earth*, *108*(B4), 2199, doi:10.1029/2001JB000682

Gasperini, P., & Ferrari, G., (2000), Deriving numerical estimates from descriptive information: The computation of earthquake parameters. *Annali di Geofisica, 43(4)*, 729–746. DOI: 10.4401/ag-3670

Guidoboni, E., & Comastri, A., 2005. Catalogue of earthquakes and tsunamis in the Mediterranean area from the 11th to the 15th century. INGV-SGA, Bologna, 1037 pp.

Guidoboni, E., Bernardini, F., & Comastri, A., (2004a), The 1138–1139 and 1156–1159 destructive seismic crises in Syria, south-eastern Turkey and northern Lebanon. *Journal of Seismology, 8*, 105–127. https://doi.org/10.1023/B:JOSE.0000009502.58351.06

Guidoboni, E., Bernardini, F., Comastri, A., & Boschi, E., (2004b), The large earthquake on 29 June 1170 (Syria, Lebanon, and central southern Turkey). *Journal of Geophysical Research: Solid Earth, 109*, B07304, doi:10.1029/2003JB002523

Guidoboni E., Ferrari G., Mariotti D., Comastri A., Tarabusi G., Sgattoni G., et al., (2018), CFTI5Med, Catalogo dei Forti Terremoti in Italia (461 a.C.-1997) e nell'area Mediterranea (760 a.C.-1500). Istituto Nazionale di Geofisica e Vulcanologia (INGV). doi: https://doi.org/10.6092/ingv.it-cfti5

Guidoboni E., Ferrari G., Tarabusi G., Sgattoni G., Comastri A., Mariotti D., et al., (2019), CFTI5Med, the new release of the catalogue of strong earthquakes in Italy and in the Mediterranean area, Scientific Data 6, Article number: 80 (2019). doi: https://doi.org/10.1038/s41597-019-0091-9

Gülerce, Z., Tanvir Shah, S., Menekşe, A., Arda Özacar, A., Kaymakci, N., & Önder Çetin, K. (2017), Probabilistic seismic-hazard assessment for East Anatolian fault zone using planar fault source models. *Bulletin of the Seismological Society of America*, *107*(5), 2353-2366. https://doi.org/10.1785/0120170009

Gürboğa, S., and Gökçe, O., (2019), Paleoseismological catalog of Pre-2012 trench studies on the active faults in Turkey. *Bulletin of Mineral Research and Exploration, 159*, 63–87. http: //dx.doi.org/10.19111/bulletinofmre.561925

Güvercin, S. E., Karabulut, H., Konca, A. Ö., Doğan, U., & Ergintav, S., (2022), Active seismotectonics of the East Anatolian Fault. *Geophysical Journal International*, *230*(1), 50–69. https://doi.org/10.1093/gji/ggac045

Hubert-Ferrari, A., Barka, A., Jacques, E., Nalbant, S. S., Meyer, B., Armijo, R., et al. (2000), Seismic hazard in the Marmara Sea region following the 17 August 1999 Izmit earthquake. *Nature, 404*, 269–273. https://doi.org/10.1038/35005054

Hubert-Ferrari, A., King., G., Manighetti, I., Armijo, R., Meyer, B., & Tapponnier, P., (2003), Long-term elasticity in the continental lithosphere; modelling the Aden Ridge propagation and the Anatolian extrusion process. *Geophysical Journal International, 153*, 111–132. https://doi.org/10.1046/j.1365-246X.2003.01872.x

Hubert-Ferrari, A., Lamair, L., Hage, S., Schmidt, S., Çağatay, M.N., & Avsar, U., (2020), A 3800 yr paleoseismic record (Lake Hazar sediments, eastern Turkey): Implications for the East Anatolian Fault seismic cycle. *Earth and Planetary Science Letters, 538*, 11615. https://doi.org/10.1016/j.epsl.2020.116152

Karakhanian, A. S., Trifonov, V. G., Ivanova, T. P., Avagyan, A., Rukieh, M., Minini, H., et al., (2008), Seismic deformation in the St. Simeon Monasteries (Qal'at Sim'an), Northwestern Syria. *Tectonophysics*, 453, 122–147. doi:10.1016/j.tecto.2007.03.008

Khair, K., Karakaisis, G. F., & Papadimitriou, E., (2000), Seismic zonation of the Dead Sea transform fault area. *Annali di Geofisica, 43(1)*, 61–79. DOI: 10.4401/ag-3620

King, G. C. P., Stein, R. S. & Lin, J., (1994), Static stress changes and the triggering of earthquakes. *Bulletin of the Seismological Society of America, 84*, 935–953. https://doi.org/10.1785/BSSA0840030935

878 Kondorskaya, R. N. V. & Ulomov, V. I., (1999), Special Catalogue of Earthquakes of
879 Northern Eurasia (SECNE) from Ancient Times through 1995. Joint Institute of
880 Physics of the Earth (JIPE), Russian Academy of Sciences, Moscow.
881 Lefevre, M., Klinger, Y., Al-Qaryouti, M., Le Béon, M., & Moumani, K., (2018), Slip deficit
882 and temporal clustering along the Dead Sea fault from paleoseismological
883 investigations. *Scientific reports*, *8*(1), 4511. https://doi.org/10.1038/s41598-018-
884 22627-9
885 Marco, S., & Klinger, Y., (2014), Review of on-fault palaeoseismic studies along the Dead
886 Sea Fault. *Dead Sea transform fault system: Reviews*, 183–205. DOI: 10.1007/978-
887 94-017-8872-4_7
888 McCaffrey, R., (2008), Global frequency of magnitude 9 earthquakes. *Geology, 36(3)*, 263–
889 266. doi: 10.1130/G24402A.1
890 Meghraoui, M., (2015), Paleoseismic History of the Dead Sea Fault Zone. In M. Beer, I. A.
891 Kougioumtzoglou, E. Patelli, & I. S.-K. Au (Eds.), *Encyclopedia of Earthquake*
892 *Engineering*, Springer-Verlag Berlin, Heidelberg. https://doi.org/10.1007/978-3-642-
893 36197-5_40-1
894 Meghraoui, M., Gomez, F., Sbeinati, R., Van der Woerd, J., Mouty, M., Darkal, A. N., et al.,
895 (2003), Evidence for 830 years of seismic quiescence from palaeoseismology,
896 archaeoseismology and historical seismicity along the Dead Sea fault in Syria. *Earth*
897 *and Planetary Science Letters, 210*, 35–52. https://doi.org/10.1016/S0012-
898 821X(03)00144-4
899 Ou, Q., Lazecky, M., Watson, C.S., Maghsoudi, Y., & Wright, T., (2023), 3D Displacements
900 and Strain from the 2023 February Turkey Earthquakes, version 1. NERC EDS
901 Centre for Environmental Data Analysis, *14 March 2023*. [Dataset]
902 https://dx.doi.org/10.5285/df93e92a3adc46b9a5c4bd3a547cd242
903 Öztürk, S., (2021), Spatio-temporal Analysis on the Aftershocks of January 24, 2020, M_w6.8
904 Sivrice- Elazığ (Turkey) Earthquake. PACE-2021 International Congress on the
905 Phenomenological Aspects of Civil Engineering, 20-23 June 2021, Atatürk
906 University, Erzurum, paper 364.
907 Papathanassiou, G., Pavlides, S., Christaras, B., & Pitilakis, K., (2005), Liquefaction case
908 histories and empirical relations of earthquake magnitude versus distance from the
909 broader Aegean region. *Journal of Geodynamics, 40(2–3)*, 257–78.
910 https://doi.org/10.1016/j.jog.2005.07.007

Perinçek, D., & Çemen, I., (1990), The structural relationship between the East Anatolian and Dead Sea fault zones in southeastern Turkey. *Tectonophysics, 172,* 331–340. https://doi.org/10.1016/0040-1951(90)90039-B

Philibosian, B., & Meltzner, A. J., (2020), Segmentation and supercycles: A catalog of earthquake rupture patterns from the Sumatran Sunda Megathrust and other well-studied faults worldwide. *Quaternary Science Reviews*, *241*, 106390. https://doi.org/10.1016/j.quascirev.2020.106390

Pousse-Beltran, L., Nissen, E., Bergman, E. A., Cambaz, M. D., Gaudreau, É., Karasözen, E., et al., (2020), The 2020 M_w 6.8 Elazığ (Turkey) earthquake reveals rupture behavior of the East Anatolian Fault. *Geophysical Research Letters, 47*, e2020GL088136. https://doi.org/10.1029/2020GL088136

Reitman, N. G., Briggs, R. W., Barnhart, W. D., Thompson Jobe, J. A., DuRoss, C. B., Hatem, A. E., et al., (2023), Preliminary fault rupture mapping of the 2023 M_w 7.8 Türkiye Earthquakes. [Dataset] https://doi.org/10.5066/P985I7U2

Rosakis, A., Abdelmeguid, M., & Elbanna, A., (2023), Evidence of Early Supershear Transition in the M_w 7.8 Kahramanmaraş Earthquake From Near-Field Records. *EarthArXiv* [preprint] https://doi.org/10.31223/X5W95G, 17 February 2023.

Rukieh, M., Trifonov, V. G., Dodonov, A. E., Minini, H., Ammar, O., Ivanov, T. P., et al., (2005), Neotectonic map of Syria and some aspects of Late Cenozoic evolution of the northwestern boundary zone of the Arabian plate. *Journal of Geodynamics, 40*, 235–256. doi:10.1016/j.jog.2005.07.016

Salamon, A., (2008), Patterns of aftershock sequences along the Dead Sea Transform - Interpretation of historical seismicity. *Geological Survey of Israel, Report GSI/05/2008*, 78 pp.

Salditch, L., Stein, S., Neely, J., Spencer, B.D., Brooks, E.M., Agnon, A., et al., (2020), Earthquake supercycles and long-term fault memory. *Tectonophysics, 774*, 228289. https://doi.org/10.1016/j.tecto.2019.228289

Satılmış, S., (2016), 1893 Malatya Earthquake and Disaster Management. *Journal Of The Center For Ottoman Studies Ankara University, 39*, 137-177.

Sbeinati, M. R., Darawcheh, R. & Mouty, M., (2005), The historical earthquakes of Syria: an analysis of large and moderate earthquakes from 1365 B.C. to 1900 A.D. *Annals of Geophysics, 47*, 733-758.

Sbeinati, M. R., Meghraoui, M., Suleyman, G., Gomez, F., Grootes, P., Nadeau, et al., (2010), Timing of earthquake ruptures at the Al Harif Roman aqueduct (Dead Sea

945 fault, Syria) from archaeoseismology and paleoseismology. In M. Sintubin, I. S.
946 Stewart, T. M. Niemi, & E. Altunel (Eds.), *Ancient Earthquakes: Geological Society*
947 *of America Special Paper 471*, p. 243–267, doi: 10.1130/2010.2471(20)
948 Seyrek, A., Demir, T., Pringle, M.S., Yurtmen, S., Westaway, R.W.C., Beck, A., et al.,
949 (2007), Kinematics of the Amanos Fault, southern Turkey, from Ar/Ar dating of
950 offset Pleistocene basalt flows: transpression between the African and Arabian plates.
951 In W. D. Cunningham, & P. Mann (Eds), *Tectonics of Strike-Slip Restraining and*
952 *Releasing Bends. Geological Society, London, Special Publications, 290*, 255–284.
953 DOI: 10.1144/SP290.9
954 Seyrek, A., Demir, T., Westaway, R., Guillou, H., Scaillet, S., White, T. S., et al., (2014),
955 The kinematics of central-southern Turkey and northwest Syria revisited.
956 *Tectonophysics, 618*, 35–66. http://dx.doi.org/10.1016/j.tecto.2014.01.008
957 Stein, R. S., Barka, A. A., & Dieterich, J. H., (1997), Progressive failure on the North
958 Anatolian fault since 1939 by earthquake stress triggering. *Geophysical Journal*
959 *International*, *128*(3), 594–604. https://doi.org/10.1111/j.1365-246X.1997.tb05321.x
960 Taftsoglou, M., Valkaniotis, S., Karantanellis, E., Goula, E., & Papathanassiou, G., (2023),
961 Preliminary mapping of liquefaction phenomena triggered by the February 6 2023
962 M7.7 earthquake, Türkiye / Syria, based on remote sensing data. Zenodo,
963 doi:10.5281/zenodo.7668400
964 Tozer, B., Sandwell, D. T., Smith, W. H. F., Olson, C., Beale, J. R., & Wessel, P., (2019),
965 Global Bathymetry and Topography at 15 Arc Sec: SRTM15+. *Earth and Space*
966 *Science, 6(10)*, 1847–1864. [Dataset] https://doi.org/10.1029/2019EA000658
967 U.S. Geological Survey, (2023), Earthquake Lists, Maps, and Statistics. Accessed March 26,
968 2023 at URL https://www.usgs.gov/natural-hazards/earthquake-hazards/lists-maps-
969 and-statistics
970 Wan, Y., Shen, Z.-K., Bürgmann, R., Sun, J., & Wang, M., (2017), Fault geometry and slip
971 distribution of the 2008 M_w 7.9 Wenchuan, China earthquake, inferred from GPS and
972 InSAR measurements. *Geophysical Journal International*, 208, 748-766. doi:
973 10.1093/gji/ggw421
974 Wells, D. L., & Coppersmith, K. J., (1994), New empirical relationships among magnitude,
975 rupture length, rupture width, rupture area, and surface displacement. *Bulletin of the*
976 *Seismological Society of America*, *84*(4), 974 – 1002.
977 https://doi.org/10.1785/BSSA0840040974

978 Wessel, P., Luis, J. F., Uieda, L., Scharroo, R., Wobbe, F., Smith, W. H. F., et al., (2019),
979 The Generic Mapping Tools version 6. *Geochemistry, Geophysics, Geosystems*, 20,
980 5556–5564. https://doi.org/10.1029/2019GC008515
981 Westaway, R., (2004), Kinematic consistency between the Dead Sea Fault Zone and the
982 Neogene and Quaternary left-lateral faulting in SE Turkey. *Tectonophysics*, *391*(1-4),
983 203-237. https://doi.org/10.1016/j.tecto.2004.07.014
984 Yönlü, Ö., (2012), Late Quaternary Activity of The East Anatolian Fault Zone Between
985 Gölbaşı (Adıyaman) And Karataş (Adana). Doctoral dissertation, Dept. of Geological
986 Engineering, Eskişehir Osmangazi Üniversitesi, June 2012 (in Turkish).
987 Zelenin, E., Bachmanov, D., Garipova, S., Trifonov, V., & Kozhurin, A., (2022), The Active
988 Faults of Eurasia Database (AFEAD): the ontology and design behind the continental-
989 scale dataset. *Earth System Science Data, 14*, 4489-4503. [Dataset]
990 https://doi.org/10.5194/essd-14-4489–2022
991

992 **Table 1.** Mentions of "East Anatolian fault" (EAF) versus "North Anatolian fault" (NAF) in
993 the title of publications from four major bibliographical databases.
994

Source[a]	EAF	NAF	Ratio NAF/EAF	Time range[b]
GeoRef	120	951	7.9	1972 – Oct. 2023
Google Scholar	238	1480	6.2	1969 – Oct. 2023
Scopus	67	447	6.3	1975 – Oct. 2023
Web of Science Core Collection[c]	74	385	5.2	1975 – Oct. 2023

995

996 [a] Except for GeoRef, which is specific for geosciences, and Google Scholar, which cannot be
997 filtered, the other two sources were filtered to include only geosciences-relevant fields.
998 [b] Start time is the year of the first publication about either fault in the database.
999 [c] Five of the EAF publications were added between April and October 2023, and concern the
1000 two 2023 major earthquakes.
1001

1002 **Table 2.** List of earthquakes and corresponding source faults.

Date[a]	M_w[b]	Name[a]	Rupture length (km)[b]	Aftershocks (months)	Source fault or fault segment
Feb. 06, 2023	7.8	Pazarcık	~ 310	ongoing	Amanos, Pazarcık, & Erkenek s.
Jan. 24, 2020	6.8	Elâziğ	(~ 35)	19[e]	Pütürge s.
Mar. 02, 1893	7.2 +/- 0.1	Malatya	~ 60	> 12[d]	Erkenek s.
Jan. 14, 1874	7.1	Sarikamiş	~ 45	≥ 12[f]	Palu s.
Apr. 03, 1872	7.2	Amik Gölu	~ 50	10[c]	Kirikhan s. & Antakya f. z.
Aug. 13, 1822	7.5	Southeastern Anatolia	~ 110	30[c]	Yesemek f. & Qanaya-Babatorun f.
Jan. 21, 1626	7.2	Hama	~ 50	unknown	northern St. Simeon f.
1513/1514	≥ 7.4	Malatya	≥ 80	unknown	Pazarcık & Nurdağı s.
Dec. 29, 1408	7.0	Shugr-Bekas	~ 40	unknown	Qanaya-Babatorun f.
Feb. 20, 1404	≥ 7.0	Aleppo	≥ 40	≥ 9[f,g]	Nusayriyah f.
Jun. 29, 1170	7.3 – 7.4	Shaizar	~ 80	4[c]	Missyaf f.
Aug. 12, 1157	7.2	Apamea	~ 50	21[c]	Shaizar f.
Oct. 11, 1138	7.2	Atharib	~ 50	8[c]	northern St. Simeon f.
Nov. 29, 1114	≥ 7.2	Antioch, Maraş	≥ 50	5[f]	Pazarcık s.

1003

1004 [a]Ambraseys (2009), except for events from 2020 (Çetin et al. 2020) and 2023 (U.S.
1005 Geological Survey, 2023).
1006 [b] For most of the earthquakes, we have estimated surface rupture lengths based on Wells &
1007 Coppersmith (1994), unless lengths were reported in original sources (discussion in text). The
1008 magnitude reported here is our preferred one among the sources discussed in the text. For the
1009 Elâziğ earthquake the rupture length value is in brackets because it did not rupture at the
1010 surface, though it had shallow slip (Pousse-Beltran et al., 2020).
1011 [c] Salamon, 2008; [d]Satılmış, 2016; [e]Öztürk, 2021; [f]Ambraseys, 2009
1012 [g] Not possible to really distinguish all aftershocks of 1404 from foreshocks of 1408.

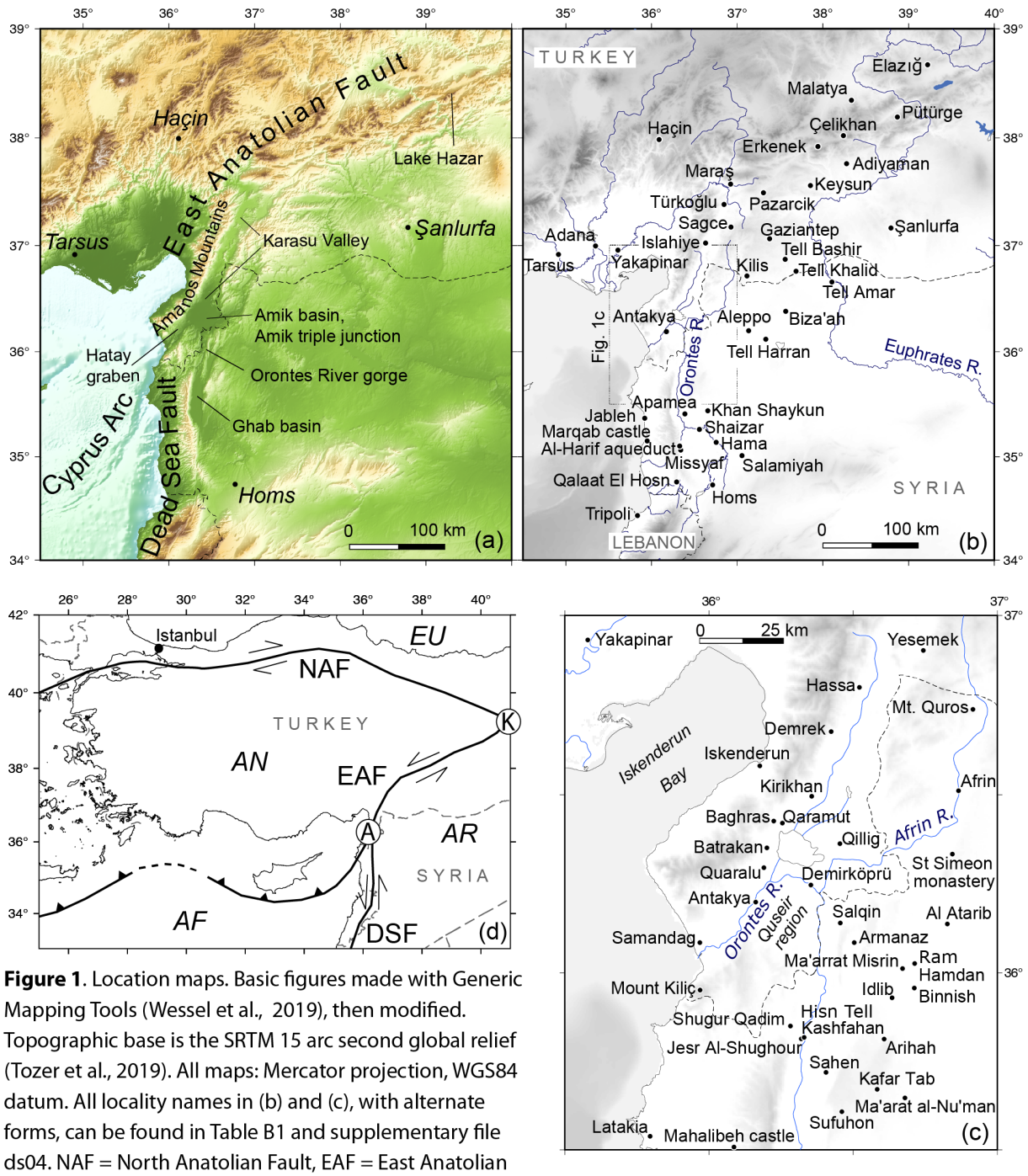

Figure 1. Location maps. Basic figures made with Generic Mapping Tools (Wessel et al., 2019), then modified. Topographic base is the SRTM 15 arc second global relief (Tozer et al., 2019). All maps: Mercator projection, WGS84 datum. All locality names in (b) and (c), with alternate forms, can be found in Table B1 and supplementary file ds04. NAF = North Anatolian Fault, EAF = East Anatolian Fault, DSF = Dead Sea Fault, K = Karliova triple junction, A = Amik triple junction; AF = African plate, AN = Anatolian plate, AR = Arabian plate, EU = Eurasian plate.

1013

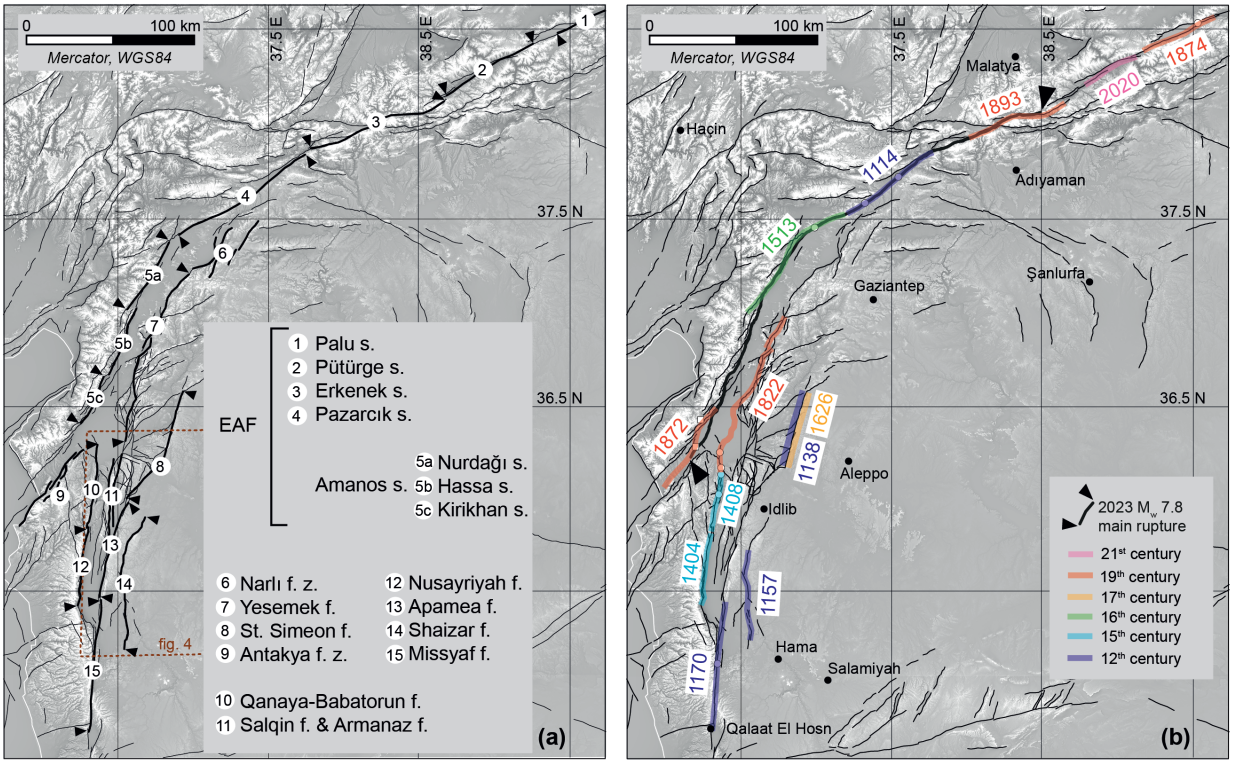

Figure 2. (a) Fault names (see Appendix B for details). The Amanos segment of the EAF is split into three further segments. Bends and stepovers are not labeled here because we do not refer to them; their names can be found in Duman & Emre (2013). s. = segment, f. = fault, f. z. = fault zone. (b) Fault rupture/earthquake pairs from Table 1. Base map and other elements are described and referenced in figure 3. Original uninterpreted base map included as supplementary file ds01, and ruptures as supplementary file ds03.

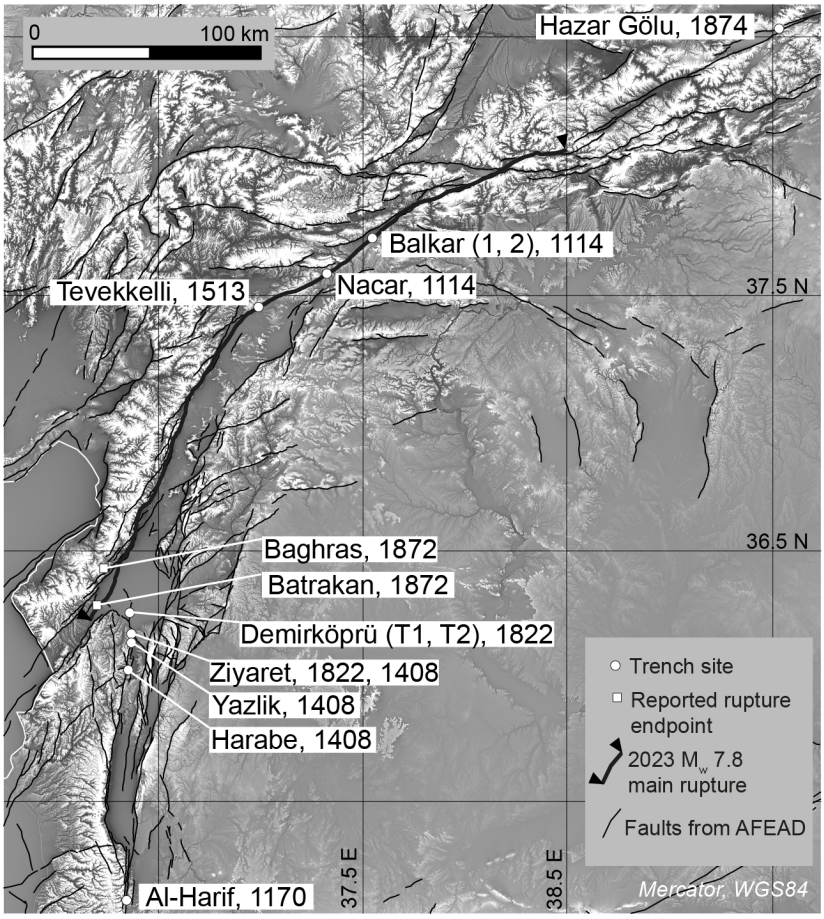

Figure 3. Location and names of trenches, and approximate historical fault rupture endpoints mentioned in the text, with the relevant pre-2023 earthquake/s indicated for each one. See references in text for each trench name. AFEAD faults are from Zelenin et al. (2022), whereas the 2023 main rupture we remapped ourselves from the pixel tracking data of Ou et al. (2023) and ForM™Ter - EOST (2023), and from the preliminary maps of Reitman et al. (2023). Basemap derived from the 30 m GLO-30 Copernicus DEM (European Space Agency, 2021), processed by applying the texture shading technique of Brown (2014).

1017

1018

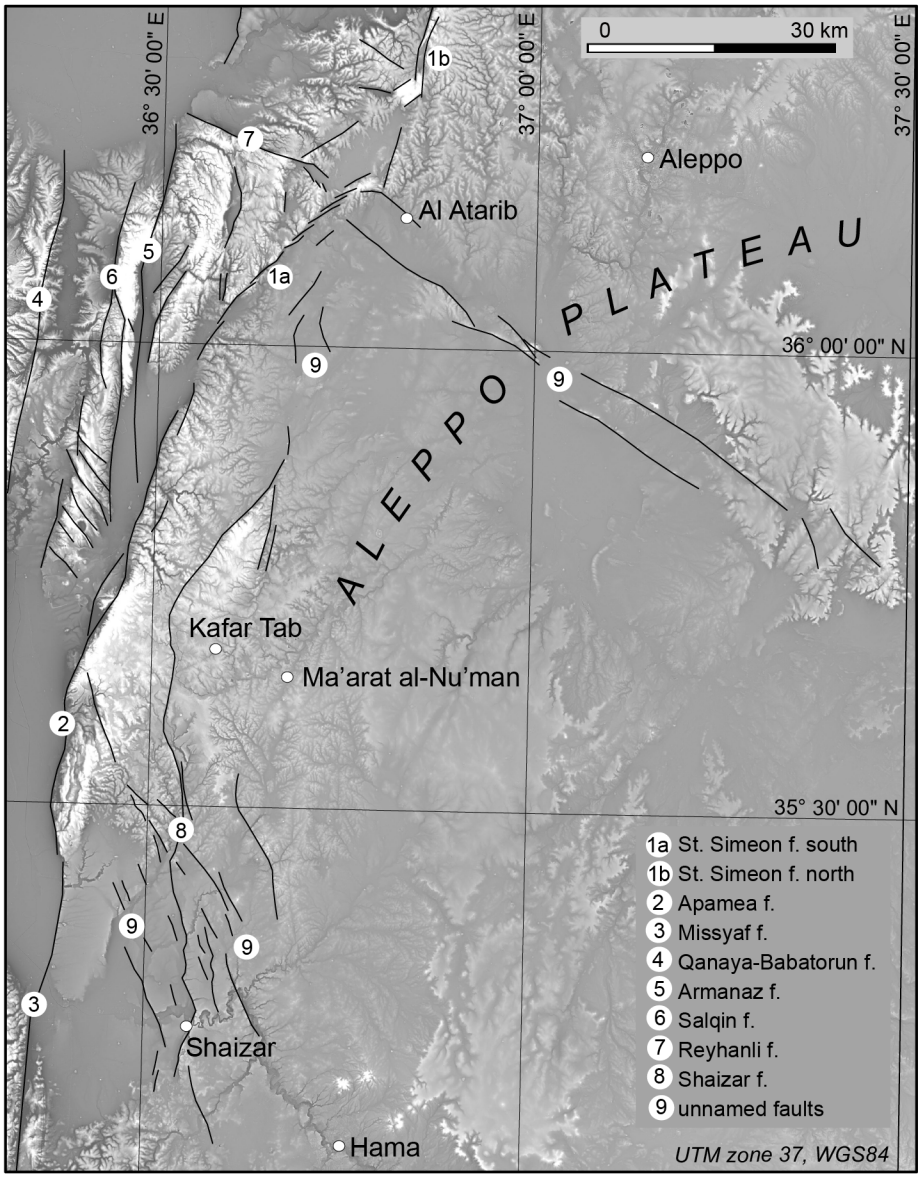

Figure 4. Faults that we mapped using the 30 m GLO-30 Copernicus DEM (European Space Agency, 2021) processed by applying the texture shading technique of Brown (2014), which can be used to enhance fine details (e.g. scarps). We mapped only the very sharpest features, which are likely to be active faults, but there are also numerous other more subtle lineaments. The background image has been muted for clarity; a full-strength and full-resolution uninterpreted image is included as a supplement (file ds02).

1019

1020

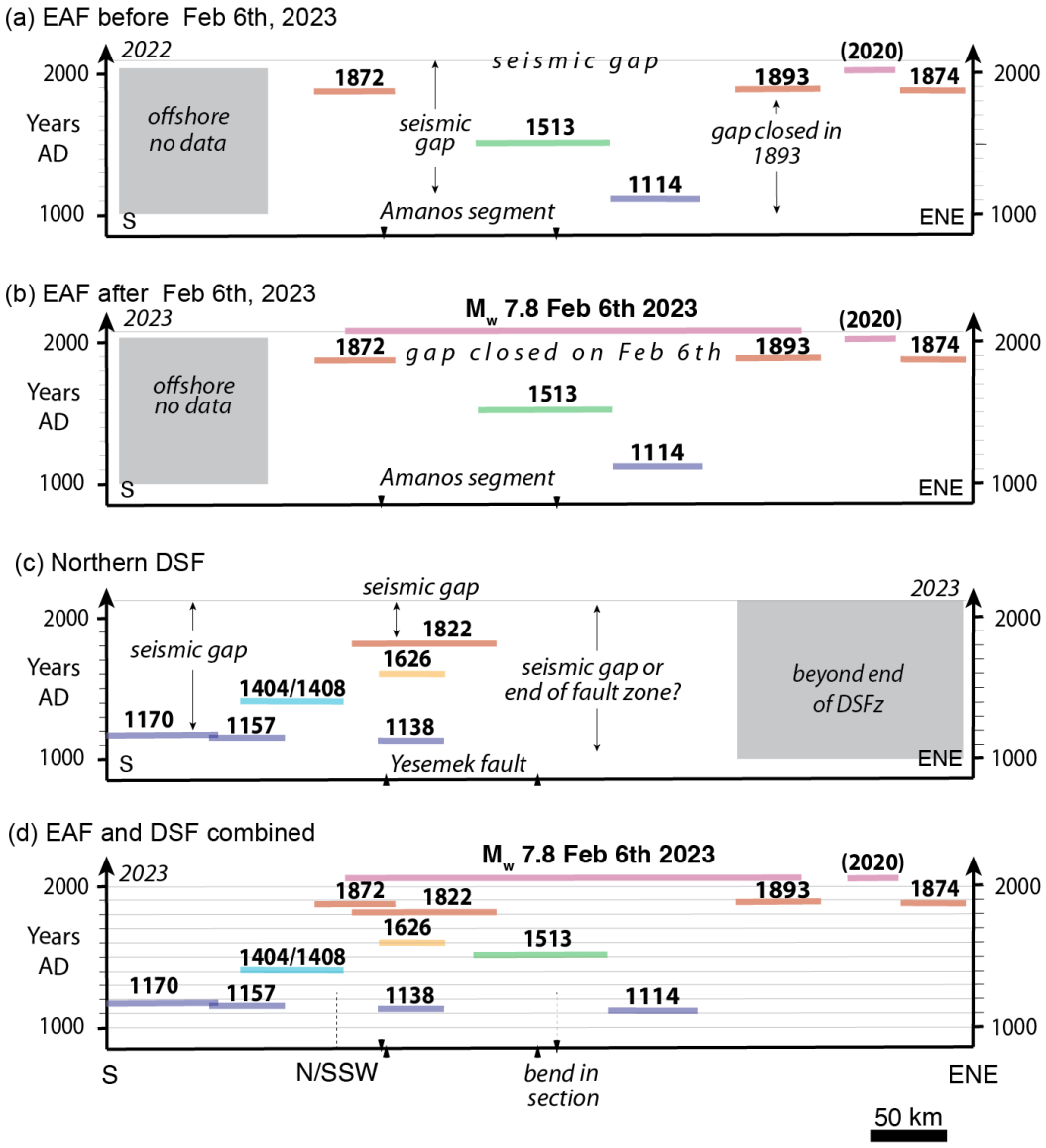

Figure 5. Space-time pattern of historic earthquakes along the EAF and northern DSF (see Figure 2 for location). The position and extent of M > 7 ruptures (horizontal bars) are justified in the text. (a and b) Pattern of M>7 ruptures for the western portion of the EAF prior to and after February 6th, 2023. (c) Pattern of M > 7 ruptures for the northern DSF. (d) Pattern of all recorded M > 7 ruptures for the region in which both active strike-slip fault systems (EAF and DSF) overlap spatially and interact kinematically.

1021

Appendix A: earthquake magnitudes

For earthquake magnitudes between 6.2 and 8.2 and depth of focus < 70 km, $M_w = M_s$ (Scordilis, 2006). As we only consider events in this magnitude range and discuss a few instrumental events for which M_w is reported, we always use M_w in our text unless it is necessary to specifically mention another type of magnitude, with the understanding that, when citing historical sources, these mostly reported either M_s determined using local empirical relationships based on rupture length, or M_F ("felt magnitude" equivalent to M_s, see below) (e.g. Ambraseys, 1988; Ambraseys & Barazangi, 1989). Another magnitude used by the INGV CIFT5Med catalog (Guidoboni et al., 2018, 2019) is M_e, which here stands for "magnitude equivalent" (i.e. equivalent to M_w) as calculated from intensities (whereas usually M_e stands for "energy magnitude" calculated from energy release) which, as far as uncertainties are concerned, we treat as M_F, because it is also fundamentally based on reported intensity areas. The difference between M_e and M_F appears to be simply the specific relationship between intensity and magnitude used, which for M_e is the one of Gasperini and Ferrari (2000). Considering that the largest source of uncertainty in estimating magnitude is the interpretation of the historical descriptions themselves, which determine what intensity is assigned to each place (for example, where one author assigns intensity X, another may assign intensity VIII), the specific relationship used does not seem to be overly important, as long as it is properly calibrated for local conditions.

To better understand this source of uncertainty, we have recalculated magnitudes ourselves for all the historical earthquakes that we considered whenever sufficient information was available, using the M_F relationship developed for Turkey by Ambraseys & Finkel (1987) and re-interpreting assigned intensities from descriptions, if necessary (especially in cases of conflicting opinions), before deciding which reported magnitude to adopt in our work:

$$M_F = -0.53 + 0.58(I_i) + 1.96\text{x}10^{-3}(R_i) + 1.83\log(R_i),$$

where R_i is the average radius (in km) of the isoseismal of intensity I_i

The reason we used M_F in our own tests instead of M_s is because not all events have a reported rupture length (which, even when reported, may be underestimated, as discussed by Ambraseys & Jackson, 1998), but nearly all have at least a "felt area". From comparing previous authors' works in this region with our own test results, the uncertainty in magnitude

1053 estimated for historical earthquakes of +/- 0.3 (Ambraseys, 1989) seems to be about right
1054 (Table A1).

1055 The addition of the 2023 events allowed us also to verify that this empirical
1056 relationship is indeed appropriate for the region, as the M_F we calculated for the two events
1057 using intensity maps from U.S. Geological Survey (2023) are 7.7 +0.2/-0.1 and 7.3 +/-0.2
1058 respectively (Table A1). Considering that different seismological laboratories in the US and
1059 Turkey (USGS, GCMT, GEOSCOPE, KOERI) have variably reported M_w of 7.7, 7.8, and
1060 8.0 for the first event, and 7.5, 7.6, and 7.7 for the second, our estimate of M_F is well within
1061 range and validates the use of this formula for older earthquakes in the region, with +/- 0.3
1062 also a reasonable, conservative uncertainty.

1063

Table A1. List of earthquakes with M_F recalculated by us, and all magnitudes reported by previous authors[a].

Date[b]	M_F	Reported magnitude[a]	Name[b]
Feb. 06, 2023	7.3 +/- 0.2	M_w 7.5, 7.6, 7.7	Elbistan
Feb. 06, 2023	7.7 +0.2/-0.1	M_w 7.7, 7.8, 8.0	Pazarcık
Jan. 24, 2020	6.6	M_w 6.7, 6.8	Elâziğ
Mar. 02, 1893	7.0	≥ 7.1; 7.2 +/- 0.1	Malatya
Jan. 14, 1874	7.0 +/- 0.1	≥ 7.1	Sarikamiş
Apr. 03, 1872	7.1 +0.2/-0.1	5.9[c]; ≤7.2; 7.2	Amik Gölu
Aug. 13, 1822	7.5 +0.3/-0.2	7.0; ≥ 7.4; 7.5	Southeastern Anatolia
Jan. 21, 1626	-	7.2	Hama
1513/1514	≥ 7.4[d]	≥ 7.4	Malatya
Dec. 29, 1408	7.1 +/- 0.1	7.0; 6 to 7; 7.4	Shugr-Bekas
Feb. 20, 1404	7.4	≥ 7.0; 7.4	Aleppo
Jun. 29, 1170	7.3 +0.2/-0.4	7.3 – 7.4; 7.3+/- 0.3; 7 to 7.8; 7.7	Shaizar
Aug. 12, 1157	7.4 +/- 0.1	7.2 +/- 0.3; 7.4	Apamea
Oct. 11, 1138	7.1 +/- 0.5	6.0; 7.5	Atharib
Nov. 29, 1114	7.3 +/- 0.4	6.9 +/- 0.3; ≥ 7.2; 7.4; ≥ 7.8	Antioch, Maraş

[a] Unless M_w is explicitly indicated, the reported magnitude is either M_s, M_F, or M_e as explained in the text.

[b] Ambraseys (2009) except for 2020 (Çetin et al., 2020) and 2023 events (U.S. Geological Survey, 2023).

[c] Sbeinati et al. (2005). It is unclear where they get this low value from, because it is very different from those of the authors they cite, and it seems to conflict with the size of the high damage area and the highest reported intensity when compared to the other events they have in the same catalog.

[d] Due to the limited information, only one intensity area can be defined, so the magnitude depends on whether this intensity is assigned as VI or VII (because significant "destruction" was reported in all localities mentioned, it should be at least VI, i.e. strong shaking).

Appendix B: fault names and place names

There seems to be no generally accepted standard about names of faults and fault segments in the region. One problem is the political border between Turkey and Syria: as it happens too often, faults (and their names) have a tendency to end or change at the border. The Active Faults of Eurasia Database (AFEAD) of Zelenin et al. (2022) often does not label the individual fault segments beyond naming the general fault zone to which they belong. For the East Anatolian fault system, we have decided to use the segment names and segment boundaries as defined in Duman & Emre (2013), because these authors go through the effort of systematically providing detailed maps, coordinates, and names in a way that is easy to follow. In the case of faults that are traditionally considered part of the Dead Sea fault system, the choice is less straightforward, because even when a fault has been labeled, its endpoints are usually ill-defined, or a vague description (e.g. "fault on the eastern side of the Ghab basin") is given, and maps in publications are small and hard to read. We chose to use the labeling of Westaway (2004) and Seyrek et al. (2012) for the following faults: Qanaya-Babatorun (called instead "Hacıpaşa segment" to the Syrian border by Akyüz et al., 2006), Nusayriyah, Apamea, Salqin, and Armanaz, which are named after nearby towns and villages. These authors also define a "East Hatay fault" on the eastern edge of the Karasu graben, whereas the same fault is called "Yesemek fault" by Duman & Emre (2013). We chose to keep the latter name because it has been assigned based on the fault going through the village of Yesemek, whereas "East Hatay" refers to a region. Finally, different authors assign the name "Afrin" (or Aafrin) fault to two entirely different faults that pass near the town of Afrin. One of these two does not appear in our analysis, but to avoid any confusion, we have decided to call the fault that we discuss "St. Simeon fault" as named by Rukieh et al. (2005) and Karakhanian et al. (2008) due to the fault passing through the St. Simeon monastery site (whereas Westaway, 2004, and Seyrek et al., 2012, call this "Afrin fault"). We were not able to find any existing names for the faults east of Apamea in Syria (on the Aleppo plateau, between the Ghab basin and Aleppo, see Figure 4), so to avoid using the "unnamed" label more than necessary, we named the largest of these "Shaizar fault", because it goes through the town bearing this name, which was destroyed in the 1157 earthquake.

Place names in this region have changed throughout the centuries depending on who controlled which territory, and even today the same name is spelled differently depending on transliteration and on native language of the writer. In reading the various publications and earthquake catalogs we had to go to some lengths to match place names from one publication

to the next, and to modern-day names that anyone can find on Google Earth. Thus, besides the standard map with locations (Figure 1), we are also including a simplified table of place names in this appendix (Table B1), plus an electronic version of it that reports all the variants we have encountered (up to six), coordinates, and any comments where needed (Supplementary file ds04). The list is by no means exhaustive, but it should help readers find their way from one publication to the next. In our paper we have decided which name to use mostly based on the primary source of our information, except for those cases where a modern name was easier to find in online searches and the name appears many times in our text (e.g. Demirköprü instead of Jisr al-Hadid). In those cases where the modern locality name has nothing to do with the one in historical records (we just matched positions between the published map and Google Earth map to identify its coordinates), we have kept the historical name in our text and maps, but supplied the name of today's nearest locality in the table (e.g. Batrakan/Atatürk).

Table B1. Place names from Figure 1, listed alphabetically in first column: in bold is the version used in text and figures. Full version in Supplementary file ds04.

Google Earth name	*Alternate name 1*	*Alternate name 2*
Afamiyah	**Apamea**	Afamea
Afrin	Aafrine	Aafrin
Al Atarib	Al-Atareb	Cerepum
Alazi	**Qaralu**	
Aleppo	Halab	Halep
Antakya	Antioch	Hatay
Armanaz	Armenhaz	
Asmacık	**Tell Khalid**	Trihalet
Atatürk	**Batrakan**	
Bakras Kalesi	**Baghras**	Bagras
Biza'ah	Bizza	
Demirköprü	Jisr al-Hadid	Jisr El Hadid
Gaziantep	Aintab	Gaziaintab
Hama	Hamat	Hamath
Haram	**Harim**	Uringa
Homs	Hims	Emesa
Iskenderun	Alexandretta	Scanderoon
Jableh	Jeble	Jabala
Jesr Al-Shughour	Jisr al-Shughur	Jisr as-Shugr
karamurt Hani	**Qaramut**	
Khan Shaykhun	Han Sheikhun	
Kharamanmaraş	**Maraş**	Germanicea
Kozkalesi	Quseyr	**Quseir**
Kumlu	**Qillig**	Quilliq
Latakia	Al-Ladhiqiya	Laodicea
Ma'arat al-Nu'man	Marre	Arra
Ma'arrat Misrin	Ma'aret Masrin	Megaret Basrin
Mahalibeh castle	Qalaat Blatnes	Balatunus
Marqab castle	Markab	Margat
Missyaf	Masyaf	Misyaf
Mount Kiliç	Mount Cassius	Al-Akraa
Orontes / Asi	Arantu	
Qalaat El Hosn	Krak (Crak, or Crac) des Chevaliers	Hisn al-Akrad
Saimbeyli	**Haçin**	Kaza Haçin
Sakcagoz	**Sagce**	Sakçagözü
Salamiyah	Salamyya	Salamiyyah
Salqin	Salqein	
Samandag	Suaidiya	Seleucia
Şanlurfa	Urfa	Edessa
Serjilla	**Kafar Tab**	Capharda
Shaizar	Shayzar	
Shugur Qadim	Castles of Shughur and Bekas	Shugr-Bekas
Tell Arn	**Tell Harran**	Tal 'Aran
Tilbasar Kalesi	**Tell Bashir**	Turbessel
Tripoli	Tarabulus	
Yakapınar	**Misis**	Mopsuestia